AD-A054 036 FLOW RESEARCH CO KENT WA F/G 20/4
NUMERICAL SOLUTIONS OF THE UNSTEADY TRANSONIC SMALL-DISTURBANCE--ETC(U)
OCT 77 M M HAFEZ, M H RIZK, E M MURMAN F33615-76-C-3067
UNCLASSIFIED FLOW-RR-83 AFFDL-TR-77-100 NL

1 OF 1
ADA
054036

END
DATE
FILMED
6-78
DDC

AFFDL-TR-77-100

NUMERICAL SOLUTIONS OF THE UNSTEADY TRANSONIC SMALL-DISTURBANCE EQUATION

FLOW RESEARCH COMPANY
A DIVISION OF FLOW INDUSTRIES, INC.
P.O. BOX 5040
KENT, WASHINGTON 98031

OCTOBER 1977

TECHNICAL REPORT AFFDL-TR-77-100
FINAL REPORT

Prepared for
AIR FORCE FLIGHT DYNAMICS LABORATORY
Air Force Wright Aeronautical Laboratories
Air Force Systems Command
Wright-Patterson Air Force Base, Ohio 45433

NOTICE

When Government drawings, specifications, or other data are used for any purpose other than in connection with a definitely related Government procurement operation, the United States Government thereby incurs no responsibility nor any obligation whatsoever; and the fact that the government may have formulated, furnished, or in any way supplied the said drawings, specifications, or other data, is not to be regarded by implication or otherwise as in any manner licensing the holder or any other person or corporation, or conveying any rights or permission to manufacture, use, or sell any patented invention that may in any way be related thereto.

This final report was submitted by Flow Research Company, A Division of Flow Industries, Inc., P.O. Box 5040 Kent, Washington 98031, under contract No. F33615-76-C3067, with the Air Force Flight Dynamics Laboratory, Wright-Patterson AFB, Ohio 45433. James J. Olsen was the Air Force Flight Dynamics Laboratory Technical Manager.

This report has been reviewed by the Information Office (OI) and is releasable to the National Technical Information Service (NTIS). At NTIS, it will be available to the general public, including foreign nations.

This technical report has been reviewed and is approved for publication.

James J. Olsen

JAMES J. OLSEN, Technical Manager
Optimization Group
Analysis and Optimization Branch

Richard D. Krobusek

RICHARD D. KROBUSEK, Maj. USAF
Chief, Analysis and Optimization Branch
Structural Mechanics Division

FOR THE COMMANDER

Howard L. Farmer

HOWARD L. FARMER, Colonel, USAF
Chief, Structural Mechanics Division

Copies of this report should not be returned unless return is required by security considerations, contractual obligations, or notice on a specific document.

(14) FLOW-RR-83

SECURITY CLASSIFICATION OF THIS PAGE (When Data Entered)

(19) **REPORT DOCUMENTATION PAGE**

READ INSTRUCTIONS BEFORE COMPLETING FORM

1. REPORT NUMBER (18) AFFDL-TR-77-100	2. GOVT ACCESSION NO.
3. RECIPIENT'S CATALOG NUMBER	
4. TITLE (and Subtitle) (6) NUMERICAL SOLUTIONS OF THE UNSTEADY TRANSONIC SMALL-DISTURBANCE EQUATIONS	5. TYPE OF REPORT & PERIOD COVERED (9) Final Report,
	6. PERFORMING ORG. REPORT NUMBER Flow Research Report No. 83
7. AUTHOR(s) (10) M. M. Hafez, M. H. Rizk, E. M. Murman, L. C. Wellford	8. CONTRACT OR GRANT NUMBER(s) (15) F33615-76-C-3067
9. PERFORMING ORGANIZATION NAME AND ADDRESS Flow Research Company, A Division of Flow Industries, Inc. P.O. Box 5040, Kent, Washington 98031	10. PROGRAM ELEMENT, PROJECT, TASK AREA & WORK UNIT NUMBERS Project: (16) 2307 (17) 05 Task: 230705 Work Unit: 23070504
11. CONTROLLING OFFICE NAME AND ADDRESS Air Force Flight Dynamics Laboratory (AFFDL/FBR) Air Force Wright Aeronautical Laboratories, AFSC Wright-Patterson AFB, OH 45433	12. REPORT DATE (11) October 1977
	13. NUMBER OF PAGES 62 (12) 68p.
14. MONITORING AGENCY NAME & ADDRESS (if different from Controlling Office)	15. SECURITY CLASS. (of this report) Unclassified
	15a. DECLASSIFICATION/DOWNGRADING SCHEDULE

16. DISTRIBUTION STATEMENT (of this Report)

Approved for public release; distribution unlimited.

61102F

17. DISTRIBUTION STATEMENT (of the abstract entered in Block 20, if different from Report)

18. SUPPLEMENTARY NOTES

19. KEY WORDS (Continue on reverse side if necessary and identify by block number)

Numerical Instabilities
Unsteady Shock Waves
Finite-Element Formulation

20. ABSTRACT (Continue on reverse side if necessary and identify by block number)

Three problems pertinent to the numerical solution of the unsteady transonic small-disturbance equation are studied. The first problem is the numerical instabilities arising in the solution of the harmonic perturbation potential equation. Several remedies that have been tested are suggested. The second problem is the movement of unsteady shock waves in the harmonic perturbation approach. A formulation and computed example are presented. The third problem is a finite-element formulation for unsteady transonic flow. Preliminary calculations are given.

DD FORM 1 JAN 73 1473 EDITION OF 1 NOV 65 IS OBSOLETE

SECURITY CLASSIFICATION OF THIS PAGE (When Data Entered)

390 409

JOB

FOREWORD

This report was prepared by Flow Research Company, A Division of Flow Industries, Inc., Kent, Washington. It was prepared for the Structural Mechanics Division of the Air Force Flight Dynamics Laboratory (AFFDL), Wright-Patterson Air Force Base, Ohio under Contract F33615-76-3067, "Numerical Solutions of the Unsteady Transonic Small Disturbance Equations". Dr. James J. Olsen of AFFDL/FBR was the Air Force Task Engineer.

At Flow Research, the principal investigator was Dr. E. M. Murman, and his associates were Dr. M. M. Hafez, Dr. M. H. Rizk, and Dr. L. C. Wellford. The report was submitted in December 1977 to cover research conducted from March 1976 through September 1977.

The authors express their appreciation to Mr. Warren Weatherill of the Boeing Company for technical discussions. The AFFDL Task Engineer expresses similar appreciation to Dr. Dennis Quinn of the Applied Mathematics Group, AFFDL/FBR.

TABLE OF CONTENTS

TABLE OF CONTENTS (CONT.)

LIST OF FIGURES

LIST OF TABLES

1. INTRODUCTION

In this report we discuss three problems associated with the numerical solution of the transonic unsteady small-disturbance equation

$$\beta\phi_{tt} + 2\phi_{xt} = (K\phi_x - \tfrac{1}{2}\phi_x^2)_x + \phi_{yy} \tag{1.1}$$

For transonic aeroelastic and flutter calculations, Weatherill et al. (1975) and Traci et al. (1975) have reported a numerical method for computing small transonic unsteady harmonic perturbations to a steady flow. The potential function is expressed in a series of increasing powers of a small parameter which measures the amplitude of an unsteady disturbance to the boundary (e.g., a thin airfoil undergoing harmonic oscillation). This results in a sequence of boundary-value problems for the perturbation potentials. The zeroth order is just the steady problem and is solved by a type-dependent finite-difference scheme with a line relaxation procedure. The first-order problem results in a linear equation of mixed type for the perturbation potential. It is solved by the same procedure.

The method of Weatherill and Traci is successful for only small, reduced frequencies. Beyond a critical frequency (for a given Mach number), the relaxation solutions diverge.

In section 2 of this report we discuss several remedies for this problem and present some computational examples.

The formulation of Weatherill and Traci does not account for the unsteady motion of the shock wave. In section 3 of this report, we discuss a method to account for this, and we present a calculated example.

The third problem we have studied is the solution of equation (1.1) by finite-element methods. An extensive review of finite-element and finite-difference methods for transonic flow was reported by Hafez, Wellford and Murman (1977).* A finite-element method for solving equation (1.1) was formulated, and it is presented in section 4. The proposed method may be used for both steady and unsteady flow problems. For steady

---

*This study was partially sponsored by NASA-Langley Research Center under contract NAS1-14246.

flow problems, the time t may be taken as an artificial time. Calculations for the steady problem are given in section 4. Calculations for the unsteady problem have not yet been completed.

2. NUMERICAL STABILITY OF THE HARMONIC APPROACH

2.1 Convergence Analysis

Weatherill et al. (1975) analyzed the convergence of the relaxation procedure for the perturbation potential.* The finite-difference approximation results in a matrix that is not always positive definite (depending on the reduced frequency). Remedies for this problem are presented in this section, and simple illustrative examples are computed. Alternative methods for solving the problem are suggested.

The Helmholtz equation was suggested by Weatherill et al. (1975) for studying the divergence of relaxation solutions that he and his colleagues encountered when solving the unsteady transonic flow equation. The Helmholtz equation

$$\phi_{xx} + \phi_{yy} + \omega^2\phi = 0 \quad , \quad \begin{matrix} 0 < x < L_1 \\ 0 < y < L_2 \end{matrix} \tag{2.1}$$

with ϕ given on the boundaries of a rectangle of length L_2 and width L_1, is simpler than the original equation, but produces similar behavior when solving it by relaxation is attempted. That is, for values of ω greater than a specific value ω_{cr}, line relaxation diverges. The one-dimensional analog to Helmholtz's equation produces the same behavior, yet it is easier to handle. For numerical illustration we shall therefore consider the boundary-value problem

---

*This linear equation is singular at the sonic line. The fundamental solutions (and the Green's functions) are different in the subsonic, sonic, and supersonic regions, and constructing the solution along these lines is a formidable task. Use of a Fourier transform in the latter direction to reduce the two-dimensional problem to a one-dimensional one will introduce convolution integrals (since the coefficients $K - \phi^o_x$ and ϕ^o_{xx} are functions of x and y). Hence, we are left with finite differences.

$$\phi_{xx} + \omega^2\phi = 0 \quad , \quad 0 < x < 1 \tag{2.2a}$$

$$\phi(0) = \phi_L \tag{2.2b}$$

$$\phi(1) = \phi_R \quad . \tag{2.2c}$$

Defining a computational net with net spacings Δx and Δy on the rectangle

$$0 < x < L_1$$
$$0 < y < L_2$$

and approximating the derivatives of equation (2.1) by central difference formulas leads to a system of algebraic equations of the form

$$A\underset{\sim}{\phi} = \underset{\sim}{f} \quad , \tag{2.3}$$

where A is the matrix of coefficients, $\underset{\sim}{\phi}$ is a vector for the unknowns at the grid points, and $\underset{\sim}{f}$ is a vector for the nonhomogeneous terms and the boundary conditions.

Trying to solve equation (2.3) by a line relaxation procedure, Weatherill et al. (1975) observed the frequency-dependent limitation on the convergence of the relaxation method. They showed that relaxation procedures converge <u>if and only if A is positive definite</u>. For fixed values of L_1, L_2, Δx, and Δy, the eigenvalues of A are functions of ω, and a critical frequency ω_{cr} for which the smallest eigenvalue is zero exists. Above this value, relaxation procedures diverge. We describe below two solutions to this problem.

2.2 Remedies to the Divergence Problem

2.2.1 The A*A Method

To solve eq. (2.3) by a relaxation procedure that converges regardless of the value of ω, we must modify the equation so that the new system matrix is positive definite. Thus, we multiply both sides of eq. (2.3) by A^*, the conjugate transpose of A, to give

$$A^*A\underset{\sim}{\phi} = A^*\underset{\sim}{f} \tag{2.4}$$

or $$A_1\underset{\sim}{\phi} = \underset{\sim}{f}_1 \ ,$$

where $$A_1 = A^*A$$

and $$\underset{\sim}{f}_1 = A^*\underset{\sim}{f} \ .$$

A_1 is positive definite except when ω is the natural frequency, in which case A is singular. If A is not singular, eqs. (2.3) and (2.4) are equivalent and have the same solution. Relaxation procedures will always converge for the new system eq. (2.4) (as long as the relaxation factor is positive and less than 2). The disadvantage of this remedy is that the bandwidth of A^*A is almost twice that of A, so that the rate of convergence may be slow. In particular, if A is ill-conditioned, A^*A will be even more so. For high frequencies the grid size must be quite small; hence, the number of equations is large, and the eigenvalues are close to each other. The smallest eigenvalue of A^*A will be very close to zero. This causes the rate of convergence to be slow.*

We demonstrate that the method described above enables us to solve the Helmholtz equation for values of ω greater than ω_{cr} by considering the one-dimensional analog to the Helmholtz equation (2.2). To solve this problem numerically, we choose a set of J discrete points x_j with uniform spacing Δx in the interval of interest $(0 < x < 1)$. We write the finite-difference approximation to equation (2.2a) at each of the points. Central-difference formulas are used to approximate the ϕ_{xx} term, and this approximation leads to the following system of algebraic equations, whose solutions approximate the solution of problem (2.2) at the set of discrete points x_j ;

$$A\underset{\sim}{\phi} = \underset{\sim}{f} \ . \tag{2.5}$$

Here, A is a tridiagonal matrix of order J ,

---

*Least-squares methods for the solutions of indefinite equations may accelerate the convergence significantly.

$$A = [1 \quad -S \quad 1] \ ,$$

$$S = 2 - \omega^2 \Delta x^2 \ ,$$

$$\underset{\sim}{f}^T = [-\phi_L \quad 0 \quad 0 \cdots 0 \quad -\phi_R] \ ,$$

where $\underset{\sim}{f}^T$ denotes the transpose of $\underset{\sim}{f}$ and where $\underset{\sim}{\phi}$ is the vector whose $\tilde{j}^{th}$ element ϕ_j approximates the solution of problem (2.2) at the point

$$x_j = j\Delta x \ .$$

The system of equations that results from multiplying eq. (2.5) by A^* is

$$A_1\underset{\sim}{\phi} \equiv A^2\underset{\sim}{\phi} = A\underset{\sim}{f} \equiv \underset{\sim}{f}_1 \ . \tag{2.6}$$

When applying the Gauss-Seidel iterative method (point relaxation) to eq. (2.6), we calculate the $n+1^{st}$ iteration with the relation

$$\phi_j^{n+1} = \phi_j^n + \Delta\phi_j^n \ , \qquad j = 1, 2, \ldots J \ ,$$

where
$$\Delta\phi_j^n = -\frac{\lambda}{a_j}\left(C_{j-2}\phi_{j-2}^{n+1} - 2SC_{j-1}\phi_{j-1}^{n+1} + a_j\phi_j^n - 2SC_{j+1}\phi_{j+1}^n + C_{j+2}\phi_{j+2}^n - \hat{f}_j\right) \ ,$$

$$j = 1, 2, \cdots J \ .$$

Here, λ is the relaxation factor,

$$a_j = \begin{cases} S^2 + 2 \ , & 2 \le j \le J-1 \\ S^2 + 1 \ , & j = 1 \ , \ J \end{cases}$$

$$C_j = \begin{cases} 1 \ , & 1 \le j \le J \\ 0 \ , & j < 1 \ , \ j > J \end{cases}$$

$$\hat{\underset{\sim}{f}}^T = \left[S\phi_L \; -\phi_L \quad 0 \quad 0 \cdots 0 \; -\phi_R \; S\phi_R \right] .$$

By numerical examples we demonstrated that relaxation, when applied to eq. (2.6), converges for those values of ω that cause it to fail when applied to eq. (2.5). In each case we calculated the direct solutions of eqs. (2.5) and (2.6). As expected, they were identical. We also obtained the exact solution of problem (2.2), and, by comparing it to the solution of eqs. (2.5) or (2.6), we were able to determine the effect of the truncation error. We applied point relaxation with $\phi_L = 0$, $\phi_R = 1$, and $J = 19$ to both systems (2.5) and (2.6). For a value of ω below π ($\omega = \pi/2$), we found that both cases converge. For a value of ω greater than π ($\omega = 3\pi/2$), we found that the iterative method converges when applied to system (2.6), but diverges when applied to system (2.5). Table I shows the results obtained for this case ($\omega = 3\pi/2$). The first column of the table gives the value of x_j at which the solution is found. The second column shows the point-relaxation (Gauss-Seidel) solution of eq. (2.6). Convergence was slow; it was achieved after 2937 iterations. Convergence is attained when the residual

$$\max_j \left| \frac{\phi_{j-1}^n - 2\phi_j^n + \phi_{j+1}^n}{\Delta x^2} + \omega^2 \phi_j^n \right| \leq 0.01 \quad , \quad j = 1, 2, \cdots, J .$$

The relaxation factor λ is equal to its optimum value 1.82. The third column of table I gives the solution of both systems (2.5) and (2.6) obtained by Gauss elimination, and the last column gives the exact solution of the boundary-value problem (2.2). The difference between the values in the last two columns is attributable to the truncation error; i.e., it is attributable to approximating the differential equation by a set of algebraic equations. As the value of ω decreases, the truncation error decreases, and the rate of convergence increases. For $\omega = \pi/2$ the difference between the exact solution and the solution of the approximating matrix equation is less than 0.02%. Moreover, convergence was achieved after 1629 iterations when equation (2.6) was solved by relaxation methods, and it was achieved after 44 iterations when equation (2.5) was solved by relaxation methods. This result indicates the

TABLE I. SOLUTION OF PROBLEM 2.2 FOR $\omega > \omega_{cr}$.

x_j	ϕ_j		
	Relaxation	Direct Inversion	Exact
0.00	0.000000	0.000000	0.000000
0.05	-.233782	-.233993	-.233445
0.10	-.454595	-.454995	-.453990
0.15	-.650187	-.650737	-.649448
0.20	-.809704	-.810353	-.809017
0.25	-.924292	-.924981	-.923880
0.30	-.987588	-.988257	-.987688
0.35	-.996073	-.996669	-.996917
0.40	-.949271	-.949749	-.951057
0.45	-.849774	-.850102	-.852640
0.50	-.703097	-.703260	-.707107
0.55	-.517377	-.517376	-.522499
0.60	-.302917	-.302769	-.309017
0.65	-.071619	-.071353	-.078459
0.70	.163678	.164024	.156434
0.75	.389914	.390295	.382683
0.80	.594527	.594898	.587785
0.85	.766155	.766474	.760406
0.90	.895265	.895499	.891006
0.95	.974685	.974808	.972370
1.00	1.000000	1.000000	1.000000

slowness of the A*A method in comparison to the usual relaxation method when it converges. In all the examples, the optimal values of the relaxation factors were used.

The above method can be extended easily to two-dimensional problems. The slowness of its convergence, however, makes it nonpractical. An alternative relaxation procedure for solving Helmholtz's equation for frequencies beyond the critical frequency is given below.

2.2.2 The Bisecting Method

For given values of ω, Δx, and Δy, there is a family of critical values L_{1cr}, L_{2cr}. For values of L_1 and L_2 outside this critical range, relaxation procedures diverge. Therefore, if we wish to solve equation (2.1) in a rectangle having dimensions beyond the critical range, we may divide the rectangle into smaller rectangles, each having dimensions below the critical values. For given values of ϕ on the boundaries of the rectangles, iteration by relaxation is certain to converge in each of them.

To solve the original problem (2.1) we are required to match the solutions in the different subregions at the internal boundaries where overlap occurs. These matches are achieved by iterating upon the boundary conditions of the subregions (the outer iteration). The inner iterations for each subregion are done by the usual relaxation method.

The above idea of dividing the original region into subregions for values of ω greater than ω_{cr} can be applied to the one-dimensional problem (2.2). Equation (2.2a) is approximated by a set of algebraic equations at J discrete points $x_j(=j\Delta x)$, $j = 1, 2, \cdots, J$ in the interval of interest P. The original interval is divided into two subintervals P_1 and P_2, each having a length below the critical length, where

$$P_1 : 0 \leq x \leq x_{JMAX1 + 1}$$

$$P_2 : x_{JMIN2 - 1} \leq x \leq 1 ,$$

and

$$JMIN2 = JMAX1 + 1 .$$

For the n^{th} outer iteration, the boundary conditions imposed on the solution for interval P_1 are

$$\phi(0) = \phi_L \tag{2.7a}$$

and

$$\phi(x_{JMAX+1}) = \psi_1^n \tag{2.7b}$$

The corresponding boundary values imposed on the solution for interval P_2 are

$$\phi(x_{JMIN2-1}) = \psi_2^n \tag{2.8a}$$

and

$$\phi(1) = \phi_R \quad . \tag{2.8b}$$

In interval P_1 M relaxation sweeps are made towards solving equation (2.2a) with boundary conditions (2.7). We then make M relaxation sweeps for solving the same equation in interval P_2, with boundary conditions (2.8) imposed. The optimal relaxation factors are used in both cases. The iterative solution at point j at the m^{th} inner iteration and the n^{th} outer iteration is denoted by $\phi_j^{m,n}$. The values for the inner boundary conditions ψ_1^n and ψ_2^n are given below. They are chosen to give the exact solution to our problem in two outer iteration steps, provided the inner iterations produce an exact solution to the problems in the subregions P_1 and P_2. The linearity of the problem is therefore exploited:

$$\psi_1^1 = C_1$$

$$\psi_1^2 = C_2$$

where C_1 and C_2 are arbitrary unequal constants.

$$\psi_1^n = \alpha^{n-1}\,\psi_1^{n-2} + (1 - \alpha^{n-1})\psi_1^{n-1}$$

$$n = 3, 4, \cdots, N$$

$$\psi_2^n = \phi_{JMAX1}^{M,n} \quad , \quad n = 1, 2, \cdots , N$$

and

$$\alpha^n = \frac{\phi_{JMIN2}^{M,n} - \psi_1^n}{(\phi_{JMIN2}^{M,n} - \psi_1^n) - (\phi_{JMIN2}^{M,n-1} - \psi_1^{n-1})}$$

The solution after the n^{th} outer iteration is given by ϕ_j^n , where

$$\phi_j^1 = \phi_j^1 \quad , \quad j = 1, 2, \cdots , J$$

$$\phi_j^n = \alpha^n \phi_j^{M,n-1} + (1 - \alpha^n)\phi_j^{M,n}$$

$$j = 1, 2, \cdots , J$$
$$n = 2, 3, \cdots , N$$

In our numerical example we have made the following specific choices

$$\phi_L = 0$$
$$\phi_R = 1$$
$$J = 19$$
$$JMAX1 = 10$$
$$JMIN2 = 11$$
$$\Delta x = 0.05$$
$$C_1 = 0$$
$$C_2 = 1 \quad .$$

The problem was solved for

$$\omega = \frac{3\pi}{2} \; (> \omega_{cr}) \quad ,$$

and the method was found to converge in a reasonable number of iterations. We assumed convergence when the residue was less than 0.01, where the residue after the n^{th} outer iteration is given by

$$\max_j \left| \frac{\phi_{j-1}^n - 2\phi_j^n + \phi_{j+1}^n}{\Delta x^2} + \omega^2 \phi_j^n \right| .$$

Table II shows the effect of changing M on the rate of convergence. To compare the rate of convergence of this method with the usual relaxation method, we calculated an example with $\omega = \pi/2$. The results are given in table III. Convergence for the usual relaxation method occurs in 44 iterations. The present method converges in only 40 iterations, when the number of inner iterations per outer iteration is 5.

The bisecting method therefore seems to be suitable for solving the problem of interest at frequencies beyond the critical value. The fact that the rate of convergence increases by reducing the number of inner iterations per outer iterations and the fast convergence demonstrated by the one-dimensional example leads us to believe in the possibility of the extension of this method to two-dimensional problems with no serious obstacles.

2.2.3 The Transform Method

We mention briefly here that J. R. Molberg (1968) developed, in his thesis, a transform technique which yields solutions to problems for which the iterative process is unstable. He used this method successfully to solve problems (2.1) and (2.2).

2.3 Other Methods for Solving Helmholtz's Equation

We have described above two modified relaxation procedures for solving the Helmholtz equation for frequencies beyond the critical frequency. These methods were suggested as remedies for the divergence problem. Other methods that can be used to solve Helmholtz's equation are described below.

2.3.1 The Shooting Method

Let us consider the one-dimensional problem (2.2). To solve this problem by the shooting method, we obtain the solutions ϕ_a and ϕ_b , each of which satisfies equation (2.2a) and initial condition (2.2b). In addition, ϕ_a and ϕ_b satisfy the initial conditions

TABLE II. NUMBER OF ITERATIONS REQUIRED FOR SOLVING PROBLEM 2.2 ($\omega > \omega_{cr}$) BY BISECTING METHOD.

Number of Outer Iterations N	Number of Inner Iterations M	N x M	Residue
1	37	37	1.3×10^{2}
2	37	74	8.8×10^{-3}
2	35	70	1.9×10^{-2}
3	35	105	6.4×10^{-7}
2	30	60	8.4×10^{-2}
3	30	90	8.4×10^{-6}
2	25	50	2.8×10^{-1}
3	25	75	2.0×10^{-4}
3	20	60	1.2×10^{-2}
4	20	80	1.4×10^{-4}
3	15	45	2.4×10^{-1}
4	15	60	7.3×10^{-3}
5	10	50	6.3×10^{-2}
6	10	60	1.7×10^{-3}
9	5	45	1.1×10^{-2}
10	5	50	5.2×10^{-3}

TABLE III. NUMBER OF ITERATIONS REQUIRED FOR SOLVING PROBLEM 2.2 ($\omega < \omega_{cr}$) BY BISECTING METHOD.

Number of Outer Iterations N	Number of Inner Iterations M	N x M	Residue
1	24	24	4.4×10
2	24	48	6.3×10^{-3}
2	20	40	1.1×10^{-1}
3	20	60	2.6×10^{-4}
3	15	45	2.0×10^{-2}
4	15	60	4.8×10^{-6}
4	10	40	2.0×10^{-2}
5	10	50	8.9×10^{-5}
7	5	35	7.5×10^{-2}
8	5	40	3.4×10^{-4}

$$\frac{d}{dx}\phi_a(0) = \beta_a \quad ,$$

$$\frac{d}{dx}\phi_b(0) = \beta_b \quad ,$$

where β_a and β_b are two arbitrary unequal constants. The desired solution ϕ of problem (2.2) is then given by

$$\phi(x) = \alpha\phi_a(x) + (1 - \alpha)\phi_b(x)$$

where $$\alpha = \frac{\phi_R - \phi_b(1)}{\phi_a(1) - \phi_b(1)} \quad .$$

The numerical scheme used to solve eq. (2.2a) is given by

$$\phi_{j+1} = (2 - \omega^2\Delta x^2)\phi_j - \phi_{j-1} \quad , \qquad j = 1, 2, \cdots, J \quad ,$$

where $$\phi_0 = \phi_L$$

and $$\phi_{-1} = \phi_1 - 2\Delta x \frac{d\phi}{dx}(0) \quad .$$

The solution obtained for ϕ by shooting is equal to that obtained by direct inversion except for round-off errors. It would appear therefore that the shooting method, which requires no iteration for the one-dimensional example, is the most attractive of all methods suggested. We point out that although the shooting method is superior to the A*A method and the bisecting method for problem (2.2), it loses some of its attractiveness in the case of the two-dimensional problem (2.1).

The two-dimensional generalization of the shooting method for solving two-point boundary value problems is only useful for small arrays because, in this method it is necessary to invert a badly ill-conditioned matrix, and the degree of ill-conditioning increases with the array size (see McAvaney et al. (1971)). A method which overcomes this difficulty was devised by Dietrick et al. (1975). It consists of dividing the region of computation into a number of small subregions. Certain boundary conditions are assumed on the interior boundaries, and

solutions are obtained in each subregion by using the generalized shooting method. An iterative process is then defined, and the values at the interior boundaries are modified after each iteration.

2.3.2 The Direct Method

We note that the finite-difference approximation to equation (2.1) may be written in the form

$$D\underset{\sim}{\phi} = \underset{\sim}{f} \quad , \tag{2.9}$$

where D is the coefficient matrix and a block tridiagonal matrix. The superdiagonal and the subdiagonal blocks are the identity matrix, and the diagonal blocks are tridiagonal matrices. A direct solution of equation (2.9) may be obtained easily by the method described by Isaacson and Keller (1966).

2.3.3 Extrapolation Method

This method avoids the unstability problems by solving eq. (2.1) for values of ω below the critical frequency. Approximate solutions for values of ω greater than the critical frequency are obtained by extrapolation. A description of this method is given in appendix A.

2.4 Concluding Remarks

Methods for solving the unsteady harmonic small-perturbation transonic flow equation have been discussed. Remedies for the divergence problem at frequencies beyond the critical frequency have been proposed, and these are shown to work by testing them on one-dimensional examples.

3. SHOCK MOVEMENT FOR THE HARMONIC APPROACH

3.1 Introduction

In this part, we investigate the problem of the shock movement caused by unsteady perturbations. In Weatherill's and Traci's work, the shock is not perturbed from the position calculated from the steady solution. For some problems, however, the shock motion is important and affects the whole flow field. To account for these effects, we derive, from a perturbation expansion for the shock-jump conditions, an equation representing the shock movement. The appropriate jumps at the unperturbed (steady) shock position are obtained by an analytical continuation of upstream and downstream conditions. To account for the shock movement, we impose the appropriate jumps on the perturbation potential with a shock-fitting procedure. A two-dimensional example is computed to illustrate the procedure.

For steady perturbations calculated by an integral equation method, Nixon (1977) has reported an alternative approach using the method of strained coordinates. In this paper we adopt the same approach for small harmonic perturbations computed by finite-difference methods. In this approach, the coordinates are strained in such a way that the shock is always fixed at its steady-state position. The perturbation of the jump conditions (in the strained coordinates) yields the same equations as the weak solution of the (linear) perturbed equation; hence, no shock fitting is necessary. The perturbed equation, however, is more complicated because it has nonhomogeneous terms accounting for the shock movement. Also, the boundary condition for the perturbed potential is altered (the airfoil is distorted so that the shock location is unchanged by the perturbation).

Finally, we show that the strained-coordinate method is equivalent to the direct method of transferring the jump conditions to the steady-state shock location.

3.2 Basic Governing Equations

The unsteady transonic small-disturbance equation can be written in the form

$$(\beta\phi_t + 2\phi_x)_t = (K\phi_x - \frac{1}{2}\phi_x^2)_x + (\phi_y)_y \,, \qquad (3.1)$$

where the ϕ_{tt} term is neglected for low frequencies. The jump conditions, admitted by the weak solution of eq. (3.1), are

$$\beta \left(\frac{\partial X^D}{\partial t}\right)^2 - 2\left(\frac{\partial X^D}{\partial t}\right) = \langle K - \phi_x \rangle + \left(\frac{\partial X^D}{\partial y}\right)^2 , \tag{3.2a}$$

$$[\![\phi]\!] = 0 , \tag{3.2b}$$

where $\langle\phi\rangle$ and $[\![\phi]\!]$ denote the average and the jump of ϕ across the shock $x = X^D(y;t)$. To complete the formulation of the problem, we must include the tangency boundary condition, a far-field behavior, and a Kutta condition for lifting airfoils.

For small harmonic perturbations, we let*

$$\phi = \phi^o(x,y) + \varepsilon \mathrm{Re}\left[e^{i\omega t}\phi^1(x,y)\right] + \varepsilon^2 \mathrm{Re}\,(\phi^{2,0} + e^{2i\omega t}\,\phi^{2,2}) + \cdots \tag{3.3}$$

where the oscillating airfoil has the following boundary condition:

$$\phi_y(x,0) = f_o'(x) + \varepsilon \mathrm{Re}\left[e^{i\omega t} f_1'(x)\right] . \tag{3.4}$$

The zeroth-order problem is given by

$$(K - \phi_x^o)\phi_{xx}^o + \phi_{yy}^o = 0 , \tag{3.5a}$$

$$\phi_y^o(x,0) = f_o'(x) , \tag{3.5b}$$

and the first-order problem (where the β term is neglected) is

$$(K - \phi_x^o)\phi_{xx}^1 + \phi_{yy}^1 - \phi_{xx}^o\phi_x^1 = 2i\omega\phi_x^1 \tag{3.6a}$$

$$\phi_y^1(x,0) = f_1'(x) . \tag{3.6b}$$

---

*This form is equivalent to $\phi = \phi^o + \tfrac{1}{2}\varepsilon(\phi^1 e^{i\omega t} + \phi^{1*} e^{-i\omega t}) + \tfrac{1}{2}\varepsilon^2(\phi^{2,0} + \phi^{2,0*} + \phi^{2,2} e^{2i\omega t} + \phi^{2,2*} e^{-2i\omega t})$.

The boundary conditions (3.5b) and (3.6b) are applied in the airfoil mean surface. Note that eq. (3.6a) is linear with discontinuous coefficients. Its solution admits jumps only at that place where the steady shocks occur. We discuss this problem below.

3.3 Equation for Shock Movement

3.3.1 Derivation of the Equation

The problem can be examined in two ways. First, we perturb the shock and transfer the perturbed jump conditions to the old position (the steady state). These transferred conditions are imposed on the perturbation potential.

In the second approach, following Nixon (1977), the method of strained coordinates is used. The coordinates are strained so that the shock is always fixed at its steady-state location (in the strained coordinates). The differential equation governing the perturbation potential, in the strained coordinates, contains nonhomogeneous terms that account for the shock movement. Also, the boundary condition is distorted. This approach is presented in section 3.4.

Following Cheng and Hafez (1973)*, the shock is perturbed in the same way the flow field is perturbed; namely, let

$$X^D(y;t) = X^o(y) + \varepsilon \mathrm{Re}\left[e^{i\omega t} X^1(y)\right] + \varepsilon^2 \mathrm{Re}\,(X^{2,0} + e^{2i\omega t} X^{2,2}) + \cdots \qquad (3.7)$$

The jump conditions (eqs. (3.2a) and (3.2b)) are given in terms of the averages and the jumps across the unknown perturbed shock $X^D(y;t)$. The appropriate jumps at the unperturbed shock $X^o(y)$ may be obtained by analytical continuation of upstream and downstream conditions. For example, consider the jump in a quantity U at X^D, namely $[\![U]\!]_{X^D}$. Up to first order, this jump can be expressed in terms of $[\![U]\!]_{X^o}$, $[\![U_x]\!]_{X^o}$ and X^1, as shown in figure 1.

---

*M. Hafez would like to thank Prof. H. K. Cheng of U.S.C. for an interesting discussion. A similar approach is studied in Cheng and Hafez (1973), where it is applied to a lift perturbation problem.

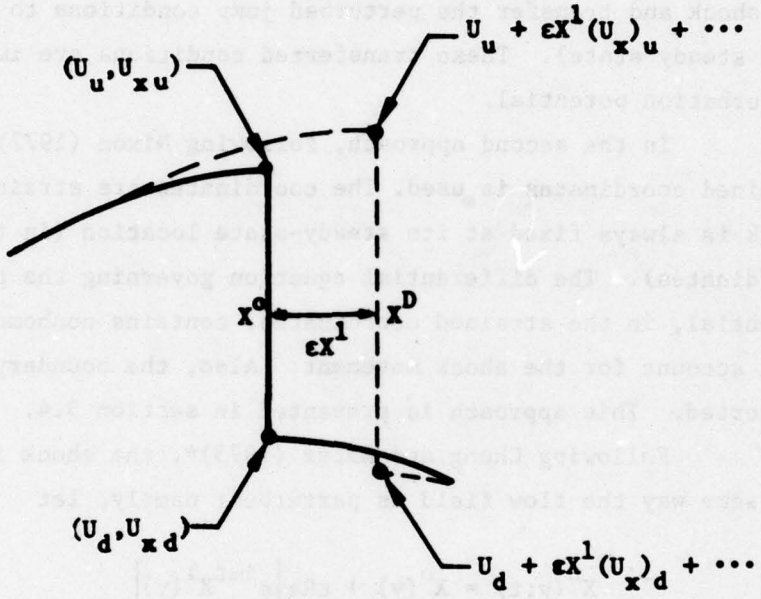

Figure 1. Perturbation of a Discontinuous Function

We can write

$$[\![U]\!]_{X^D} = U_d + \varepsilon X^1 (U_x)_d + \cdots - \left(U_u + \varepsilon X^1 (U_x)_u + \cdots\right)$$

$$= (U_d - U_u) + \varepsilon X^1 \left[(U_x)_d - (U_x)_u\right] + \cdots$$

$$= [\![U]\!]_{X^o} + \varepsilon X^1 [\![U_x]\!]_{X^o} + \cdots \ .$$

Similarly, we have $\quad \langle U \rangle_{X^D} = \langle U \rangle_{X^o} + \varepsilon X^1 \langle U_x \rangle_{X^o} + \cdots \ .$

Now, consider condition (3.2b)expanded in terms of ε :

$$[\![\phi^o + \varepsilon\phi^1 + \cdots]\!]_{X^D} = [\![\phi^o + \varepsilon\phi^1 + \cdots]\!]_{X^o} +$$

$$+ \varepsilon X^1 [\![\phi^o_x + \varepsilon\phi^1_x + \cdots]\!]_{X^o} + \cdots = 0 \ . \qquad (3.8)$$

The zeroth and first-order relations are given by,

$$\text{for } \varepsilon^o, \quad [\![\phi^o]\!]_{X^o} = 0 \ , \qquad (3.9)$$

$$\text{for } \varepsilon^1, \quad [\![\phi^1]\!]_{X^o} = -X^1 [\![\phi^o_x]\!]_{X^o} \ . \qquad (3.10)$$

Similarly, condition (3.2a) gives,

$$\text{for } \varepsilon^o, \quad \langle K - \phi^o_x \rangle_{X^o} = -\left(\frac{\partial X^o}{\partial y}\right)^2 \ , \qquad (3.11)$$

$$\text{for } \varepsilon^1, \quad 2i\omega X' = \langle \phi^1_x + X^1 \phi^o_{xx} \rangle_{X^o} - 2\,\frac{dX^o}{dy}\,\frac{dX^1}{dy} \qquad (3.12)$$

Equation (3.12) is an ordinary differential equation in X^1 . Together with eq. (3.10), it imposes the proper jump conditions on ϕ^1 . A shock-fitting procedure is necessary since the weak solution of the (linear) perturbed system (3.6) admits discontinuities other than the conditions that result from perturbing the jumps admitted by the fully nonlinear system. (3.1) To calculate the pressures in the region of the shock, we must take into account the motion of the shock as discussed in appendix B.

3.3.2 Simplification for Normal Shock*

For a locally normal shock, the term $\frac{dX^o}{dy}\frac{dX^1}{dy}$ in eq. (3.12) is neglected; hence,

$$2i\omega X^1 = \left\langle \phi_x^1 + X^1 \phi_{xx}^o \right\rangle_{X^o} . \tag{3.13}$$

Eliminating X^1 between (3.10) and (3.13), we have

$$\left\langle \phi_x^1 \right\rangle_{X^o} \left[\!\left[\phi_x^o \right]\!\right]_{X^o} + \left\langle 2i\omega - \phi_{xx}^o \right\rangle_{X^o} \left[\!\left[\phi^1 \right]\!\right]_{X^o} = 0 . \tag{3.14}$$

Equation (3.14) is the jump condition to be imposed on ϕ^1. After ϕ^1 is calculated, we can evaluate X^1 from eq. (3.13) or (3.10).

3.3.3 A Shock-Fitting Procedure for the ϕ^1 Problem

First, we solve the steady problem ϕ^o, using, for example, Murman's fully conservative schemes. From the ϕ^o solution, we let $\left[\!\left[\phi_x^o \right]\!\right]_{X^o} = a$ and $\left\langle 2i\omega - \phi_{xx}^o \right\rangle_{X^o} = b$, where X^o is considered part of the ϕ^o solution. The first point downstream of the shock X^o is identified by S.P. in figure 2. At this point, we replace the finite-difference equation for ϕ^1 by the following relation:

$$\frac{a}{2}\left(\frac{\phi_{i+1}^1 - \phi_i^1}{\Delta x} + \frac{\phi_{i-1}^1 - \phi_{i-2}^1}{\Delta x} \right) + b(\phi_i^1 - \phi_{i-1}^1) = 0 . \tag{3.15}$$

Equation (3.15) is a first-order approximation of eq. (3.14).

The shock is treated as an internal boundary with a boundary condition in the form of

$$a_1 \phi^+ + b_1 \phi_x^+ = c_1 ,$$

where a_1, b_1, and c_1 are constants, (+) denotes the conditions just downstream of the shock, and c_1 contains the conditions on the upstream side of the shock.

---

*For normal shock, $\left\langle \phi_{xx}^o \right\rangle = 0$.

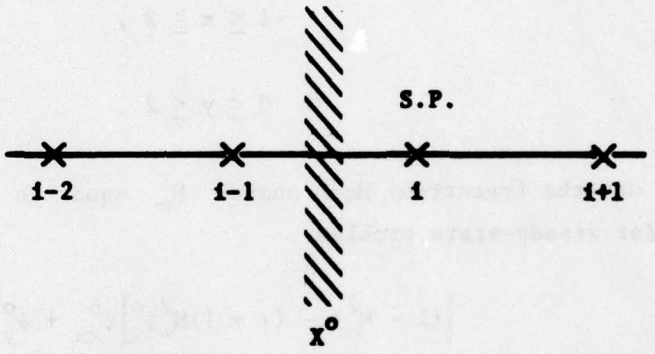

Figure 2. Shock Points and Shock Location

3.3.4 Computational Example

Using the above theory, we can compute a two-dimensional example of a pulsating parabolic arc airfoil. The airfoil is placed on the line $y = 0$, and its upper surface is governed by the equation

$$y_u = 0.2\, x\, (1 - x)(1 + 0.1 \sin \omega t) ,$$

where

$$\omega = 0.818 .$$

We now solve the problem in the rectangular domain

$$-1 \leq x \leq 2 ,$$

$$0 \leq y \leq 2 .$$

We set the freestream Mach number M_∞ equal to 0.818 and solve the lowest order steady-state problem

$$\left[(1 - M_\infty^2) - (\gamma + 1) M_\infty^2 \phi_x^o\right] \phi_{xx}^o + \phi_{yy}^o = 0$$

$$\phi^o(-1,y) = 0 \quad , \quad \phi^o(1,y) = 0$$

$$\phi^o(x,2) = 0$$

$$\phi_y^o(x,0) = \begin{cases} 0 & x < 0 \\ 0 & x > 1 \\ 0.2(1-2x) & 0 < x < 1 \end{cases}$$

by using the Murman type-dependent relaxation scheme. A plot of the solution is shown in figure 3. The unsteady perturbation equation

$$\left[(1 - M_\infty^2) - (\gamma + 1) M_\infty^2 \phi_x^o\right] \phi_{xx}^1 + \phi_{yy}^1 - \phi_x^1 \left[(\gamma + 1) M_\infty^2 \phi_{xx}^o + i2\omega\right] = 0 \qquad (3.16)$$

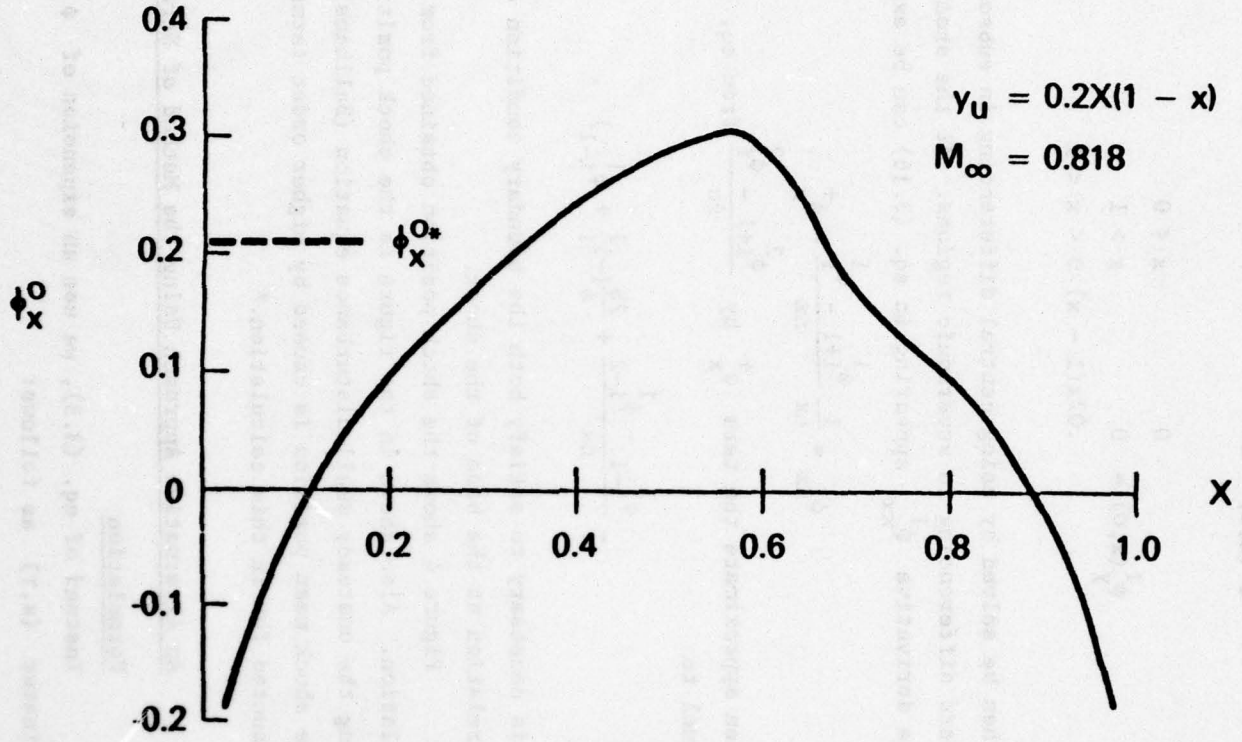

Figure 3. Steady-State Solution for a Parabolic Airfoil

with the boundary conditions

$$\phi^1(-1,y) = 0 \qquad \phi^1(1,y) = 0$$

$$\phi^1(x,2) = 0$$

$$\phi_y^1(x,0) = \begin{cases} 0 & x < 0 \\ 0 & x > 1 \\ .02x(1-x) & 0 < x < 1 \end{cases}$$

can then be solved by using central differencing in subsonic regions and backward differencing in supersonic regions. At the shock point, the double derivative ϕ_{xx}^1 appearing in eq. (3.16) can be expressed as

$$\phi_{xx}^1 = \frac{1}{\Delta x}\left(\frac{\phi_{i+1}^1 - \phi_i^1}{\Delta x} - \phi_x^+\right) .$$

We then approximate the term ϕ_x^+ by $\frac{\phi_{i+1}^2 - \phi_i^2}{\Delta x}$ from eq. (3.15) and set it equal to

$$-\frac{\phi_{i-1}^1 - \phi_{i-2}^1}{\Delta x} + \frac{2b}{a}(-\phi_i^1 + \phi_{i-1}^1) \quad .$$

This is necessary to satisfy both the boundary condition and the shock jump relation at the base of the shock.

Figure 4 shows the shock position obtained from the present calculation. Also shown in the figure is the shock position obtained by solving the unsteady small-disturbance equation (Ballhaus). The shift in the shock mean position is caused by higher order terms which are unaccounted for in this calculation.*

3.4 An Alternative Approach Using the Method of Strained Coordinates

3.4.1 Formulation

Instead of eq. (3.3), we use an expansion of ϕ in strained coordinates (s,τ) as follows:

---

*A modified quasi-steady approach may be used where the unsteady (ϕ_{xt}) term is evaluated by using the first-order perturbation solution. This approach leads to a nonhomogeneous equation of the form

$$(K - \phi_x)\phi_{xx} + \phi_{yy} = (\text{Re } 2i\omega M_\infty^2 \phi_x^1 e^{i\omega t}$$

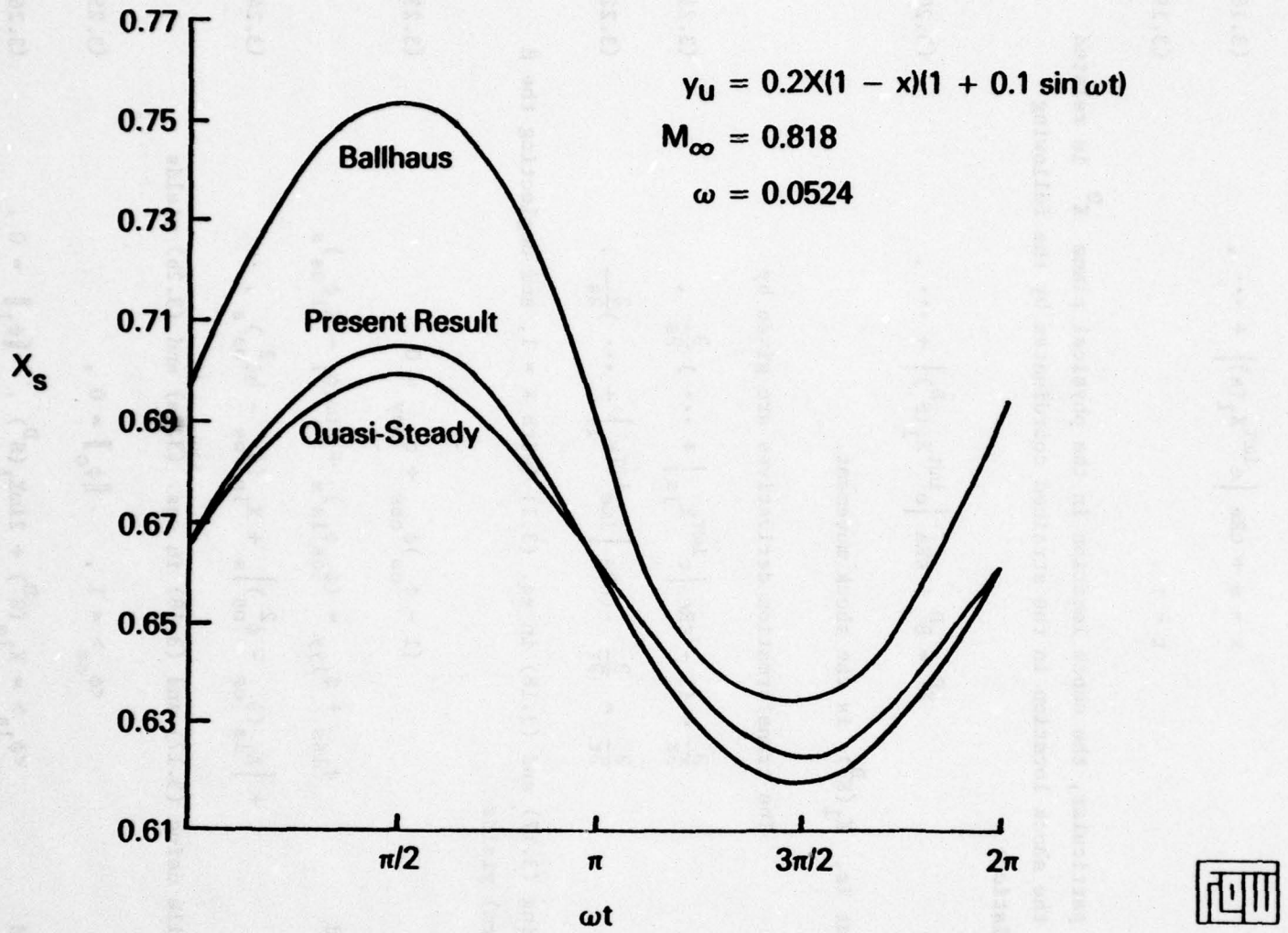

Figure 4. Shock Movement at the Surface of a Pulsating Airfoil

Let $$\phi(x,y;\tau) = \phi_o(s,y) + \varepsilon \mathrm{Re}\left[e^{i\omega\tau}\phi_1(s,y)\right] + \cdots , \tag{3.17}$$

$$x = s + \varepsilon \mathrm{Re}\left[e^{i\omega\tau}X_1(s)\right] + \cdots , \tag{3.18}$$

$$t = \tau . \tag{3.19}$$

In particular, the shock location in the physical plane X^D is related to the shock location in the strained coordinates by the following relation:

$$X^D = S^D + \varepsilon \mathrm{Re}\left[e^{i\omega\tau}X_1(S^D)\right] + \cdots . \tag{3.20}$$

That is, $X_1(S^D)$ is the shock movement.

The transformation derivatives are given by

$$\frac{\partial}{\partial x} = (1 - \varepsilon \mathrm{Re}\left[e^{i\omega\tau}X_{1s}\right] + \cdots)\frac{\partial}{\partial s} , \tag{3.21}$$

$$\frac{\partial}{\partial t} = \frac{\partial}{\partial \tau} - (\varepsilon \mathrm{Re}\left[i\omega e^{i\omega\tau}X_1\right] + \cdots)\frac{\partial}{\partial s} . \tag{3.22}$$

Using (3.17) and (3.18) in eq. (3.1) (with K = 1, and neglecting the β term) yields

$$(1 - \phi_{os})\phi_{oss} + \phi_{oyy} = 0 , \tag{3.23}$$

and $$\phi_{1ss} + \phi_{1yy} = (\phi_{os}\phi_{1s})_s + 2i\omega(\phi_1 - X_1\phi_{os})_s$$

$$+ \left[X_{1s}(\phi_{os} - \phi_{os}^2)\right]_s + X_{1s}(\phi_{os} - \tfrac{1}{2}\phi_{os}^2)_s , \tag{3.24}$$

while using (3.17) and (3.18) in eqs. (3.2a) and (3.2b) yields

$$\langle\phi_{os}\rangle = 1 , \qquad [\![\phi_o]\!] = 0 , \tag{3.25}$$

and $$\langle\phi_{1s}\rangle = X_{1s}(S^D) + 2i\omega X_1(S^D) , \quad [\![\phi_1]\!] = 0 . \tag{3.26}$$

Note that eqs. (3.25) and (3.26) are the jump conditions admitted by the weak solutions of eqs. (3.23) and (3.24), respectively. The boundary conditions in the physical plane are transformed to

$$\phi_{oy}(s,0) = W_o(s) \quad \text{on the airfoil, and} \tag{3.27}$$

$$\phi_{1y}(s,0) = W_1(s) + X_1(s)W_{os}(s) \quad \text{on the airfoil .} \tag{3.28}$$

Equations (3.23), (3.25), and (3.27) determine the steady state, while eqs. (3.24), (3.26), and (3.28) determine the perturbation potential in the strained coordinates.

3.4.2 Difference Equations

For the steady-state problem, centered differences are used in the subsonic region, backward differences in the supersonic region, a parabolic-point operator at the sonic line (to exclude expansion shock), and a shock-point operator at the shock point to impose the right jump condition (conservation of mass).

For the perturbation potential, a parabolic-point operator and a shock-point operator are needed. Also, $X_1(S_o)$ is unknown.

We first consider the parabolic-point operator. In (x,y,t) coordinates, $\phi_x = 1$ at the sonic line. To guarantee finite acceleration ϕ_{xx} at the sonic line, eq. (3.1) reduces to

$$\phi_{yy} = 2\phi_{xt} . \tag{3.29}$$

Parabolic-point operators in (s,y,τ) coordinates are given by

$$\phi_{oyy} = 0 , \tag{3.30}$$

$$\phi_{1yy} = 2i\omega(\phi_{1s} - X_{1s}\phi_{os}) . \tag{3.31}$$

In eqs. (3.30) and (3.31) centered differences are used everywhere.

Equation (3.24) at ($\phi_{os} = 1$) reads

$$(1 - \phi_{os})\phi_{1ss} = \phi_{oss}\,[\phi_{1s} - (X_{1s} + 2i\omega X_1)\,] . \tag{3.32}$$

To keep ϕ_{1ss} finite at the ($\phi_{os} = 1$), we must satisfy the following condition:

$$\phi_{1s} = X_{1s} + 2i\omega X_1 \ , \quad \text{at } \phi_{os} = 1 \ . \tag{3.33}$$

Equation (3.33) is used to determine the shock movement Δ (assuming, for example,

$$X_1(s) = \Delta s(1 - s)/S^D(1 - S^D)$$

as in Nixon's work (1977)). Note that eq. (3.33) is consistent with eq. (3.26) when the shock strength vanishes.

We next consider the shock-point operator. Equation (3.24) is written in a conservative form. A fully conservative scheme that admits the appropriate jumps eq. (3.26) is written as follows:

$$(\text{Shock-Point Operation})_i = (\text{Elliptic Operator})_i + (\text{Hyperbolic Operator})_i \ . \tag{3.34}$$

The y terms are central differenced.

After algebraic manipulation, eq. (3.34) reduces to (neglecting y terms for a locally normal shock)

$$\frac{U^+ + U^-}{2} = X_{1s}(S^D) + 2i\omega X_1(S^D) \ , \tag{3.35}$$

where

$$U^+ = \frac{\phi_{1,i+1} - \phi_{1,i}}{\Delta X} \ ,$$

$$U^- = \frac{\phi_{1,i-1} - \phi_{1,i-2}}{\Delta X} \ ,$$

Equation (3.35) is a first-order approximation of jump condition (3.26).

3.5 Equivalence of the Two Methods

Finally, we want to show that these results are consistent with the previous approach and that the two approaches are equivalent.

We substitute eq. (3.18) into eq. (3.3), together with a Taylor series expansion for ϕ^o around the point x,y, and collect terms of equal orders. The result is

$$\phi(x,y,t) = \phi^o(s,y) + \varepsilon \mathrm{Re}\left\{e^{i\omega t}\left[\phi^1(s,y) + X_1(s)\phi^o_s(s,y)\right]\right\} + \cdots . \tag{3.36}$$

Comparing eqs. (3.36) and (3.17), we find

$$\phi^o(s,y) = \phi_o(s,y) ,$$

$$\phi^1(s,y) + X_1(s)\phi^o_s(s,y) = \phi_1(s,y) . \tag{3.37}$$

The equation for $\phi^1(s,y)$ reads

$$\phi^1_{ss} + \phi^1_{yy} = (\phi^o_s \phi^1_s)_s , \tag{3.38}$$

with the boundary condition

$$\phi^1_y(s,0) = W_1(s) \tag{3.39}$$

on the airfoil and the shock-jump conditions

$$[\![\phi^1]\!] = -X_1(S^D)\,[\![\phi^o_s]\!] , \tag{3.40}$$

$$\langle\phi^1_s\rangle + X_1(S^D)\langle\phi^o_{ss}\rangle = 2i\omega X_1(S^D) . \tag{3.41}$$

Equations (3.38), (3.39), (3.40), and (3.41) were used before with a shock-fitting procedure to determine ϕ^1. Hence, the two systems are equivalent.

3.6 Conclusions

We have derived an expression for the perturbed shock position for unsteady transonic calculations. This result provides us with a consistent method for predicting the shock motion of small unsteady harmonic purturbations. A two-dimensional example has been calculated.

4. FINITE ELEMENT METHODS FOR STEADY AND UNSTEADY TRANSONIC FLOWS

4.1 Introduction

For isentropic, irrotational, transonic flows, Euler's equations reduce to the mass conservation equation. Evaluating the density from the Bernoulli (energy) equation, we find the flow is governed by a single second-order nonlinear hyperbolic equation in terms of a velocity potential. The steady equation, however, is of mixed type (i.e., locally hyperbolic (elliptic) for the supersonic (subsonic) region. The change of the type of the equation and the existence of a discontinous solution (shock waves) are attributable to the nonlinearity). It seems that the unsteady problem is more amenable to analysis. In fact, the steady solution is obtained as the steady-state limit (for large times) of the unsteady problem.

The controlling parameters, in general, are the Mach number, geometry parameters (angle of attack, thickness ratio, aspect ratio, etc.) and the unsteady disturbance parameters (frequency and amplitude). With standard limit processes, different approximations can be obtained. The most famous of these is the transonic small-disturbance theory. For the high-frequency range, the nonlinear terms can be neglected, and the equation is linear. For the low-frequency range, the nonlinear term is important, and other linear terms like the ϕ_{tt} term are not. Although the approximations lead to great simplification, some mathematical difficulties are associated with the resulting governing equation in this range (a parahyperbolic equation with one real characteristic).

The solution procedures for the unsteady problems are numerous. On one hand, the straightforward, quasi-steady approach, where time is considered a parameter, may be justifiable in the low-frequency range, if we have an efficient method for solving the steady problem. On the other hand, direct time integration of the unsteady equation allows for the full unsteady effects to take place. In between these two methods are the linear perturbation methods for small unsteady disturbances, namely, the frequency and indicial response methods. In the frequency decomposition method, a sequence of steady-like problems (for different frequencies) are solved; while, for the indicial method, the response of a linearized time-dependent equation to an impulse is calculated. As mentioned earlier in this report, perturbation of a system with a discontinuous

solution must be treated with a special consideration. Nonlinear finite-amplitude effects can be included if the main flow is allowed to interact with the disturbance leading to a coupled system of nonlinear equations for the main flow as well as the perturbations.

Numerical methods are needed to implement these procedures. In the following sections, application of the finite-element method to the steady and unsteady transonic problems is studied.

In recent years various finite-element techniques have been developed for steady small-disturbance transonic flow problems. Chan, Brashears, and Young (1975) presented the first application of finite-element methods in transonic flow. They resorted to a least-squares model after discovering that Galerkin formulations, in conjunction with an iterative scheme based on a sequence of Poisson solutions, did not converge for supercritical flows. Wellford and Hafez (1976) constructed a workable Galerkin model by introducing a mixed variational principle and an appropriate direct-gradient solution algorithm. Hafez, Murman, and Wellford (1976) developed a Galerkin model that accounted for the change in type of the differential equation in a manner similar to the technique used in Murman's original work. Glowinski, Periaux, and Pironneau (1976) introduced an optimal control formulation for transonic flow. The finite-element method has not been used for unsteady transonic flows however, there is some work in the literature on the solution of shallow water equations, which are similar to the transonic equation ($\gamma=2$).

In the present study, we have constructed an alternate Galerkin model for the small-disturbance transonic problem and have developed a solution algorithm for the resulting equations. The problem is formulated in terms of velocities, and an implicit finite element is constructed by using the time-dependent model of Magnus and Yoshihara (1970) for both steady and unsteady problems. Because the resulting algorithm is essentially independent of the type of the flow (subsonic or supersonic), it is well suited for finite-element models. Curved boundary shapes and irregular meshes can be used. The advantages of the finite-element method in modeling highly irregular domains and in incorporating higher order accurate elements can therefore be utilized.

In the following sections the physical problem is posed, the iterative solution algorithms are introduced, the convergence criteria for the solution algorithm are determined, and numerical results are presented.

4.2 The Physical Problems

We consider the flow of an inviscid, compressible fluid about a thin airfoil. We adopt here the small-disturbance theory (see Landahl (1961)). Let Ω be an infinite domain composed of points (x,y). Let $\overline{\Omega}$ be the upper half plane defined by $y \geq 0$, for all x. We consider non-lifting symmetric flows, and thus we model domains Ω such that $\Omega \subseteq \overline{\Omega}$. Ω is the same as $\overline{\Omega}$ except for the region occupied by the airfoil. We describe the boundary $\partial\Omega_1$ of the upper half plane of the symmetric airfoil by $y = g(x,t)$ where $y = 0$ is the chord of the airfoil. The boundary $\partial\Omega_2$ of the flow is the boundary $(y = 0)$ of the halfplane $\overline{\Omega}$ for points outside the airfoil. The boundary $\partial\Omega_3$ of the flow is the boundary of the halfplane at ∞ in the y direction. The boundary $\partial\Omega_4$ of the flow is the boundary of the halfplane at $x = \infty$ and $x = -\infty$. The boundary $\partial\Omega$ of Ω is $\partial\Omega = \partial\Omega_1 \cup \partial\Omega_2 \cup \partial\Omega_3 \cup \partial\Omega_4$.

Let ϕ be the perturbation velocity potential, M_∞ be the free-stream Mach number, and γ be the ratio of specific heats. Then the problem is described by the following set of equations:

$$\left[(1-M_\infty^2)\phi_{,x} - \frac{M_\infty^2(1+\gamma)\phi^2}{2}{}_{,x}\right]_{,x} + \phi_{,yy} = 2M_\infty^2\phi_{xt} + M_\infty^2\phi_{tt} \text{ in } \Omega$$

$$g_t + (1 + \phi_{,x})g_{,x} - \phi_{,y} = 0 \quad \text{on } \partial\Omega_1 \tag{4.1}$$

$$\phi_{,y} = 0 \quad \text{on } \partial\Omega_2$$

$$\nabla\phi = 0 \quad \text{on } \partial\Omega_3 \cup \partial\Omega_4$$

For steady flows, suppose that the x and y velocity components are defined by $u = \phi_{,x}$ and $v = \phi_{,y}$. Then (4.1) can be written in the following form (a system of first-order equations):

$$\left[K_1 u - \frac{K_2}{2} u^2\right]_{,x} + v_{,y} = 0 \qquad \text{in } \Omega$$

$$(1 + u)g_{,x} - v = 0 \qquad \text{on } \partial\Omega_1$$

$$v = 0 \qquad \text{on } \partial\Omega_2 \cup \partial\Omega_3 \tag{4.2}$$

$$u = 0 \qquad \text{on } \partial\Omega_4$$

where $K_1 = 1 - M_\infty^2$ and $K_2 = (1 + \gamma)M_\infty^2$. Irrotationality is imposed by requiring that

$$u_{,y} - v_{,x} = 0 \qquad \text{in } \Omega \ . \tag{4.3}$$

The low-frequency unsteady equation (omitting the ϕ_{tt} term) is a system of first-order equations in the form of:

$$(K_1 u - \frac{K_2}{2} u^2)x + v_y = \alpha u_t$$

$$u_y - v_x = 0 \tag{4.4}$$

The high-frequency equation (4.1), can be written, however, in the form of a system of first-order equations if we use three variables u, v and w where $w = \phi_t$; namely,

$$(K_1 u - \frac{K_2}{2} u^2)_x + v_y - 2\alpha w_x = w_t$$

$$w_x = u_t \tag{4.5}$$

$$w_y = v_t$$

where $K_1 = 1 - M_\infty^2$ and $K_2 = (1+\gamma)M_\infty^2$. Irrotationality is imposed by requiring that

$$u_y - v_x = 0 \qquad \text{in } \Omega \ .$$

4.3 Tentative Solution Algorithms

To construct a workable solution algorithm, we introduce time-dependent and explicit artificial viscosity terms as follows:

$$\alpha u_{,t} = \left[K_1 u - \frac{K_2}{2} u^2\right]_{,x} + v_{,y}$$

$$+ \gamma u_{,xx} - \chi u \tag{4.6}$$

$$\beta v_{,t} = u_{,y} - v_{,x} + \lambda v_{,yy} - Fv \ .$$

Of course, the second-order terms in (4.6) can be associated with viscous dissipation. The terms involving u and v are more difficult to explain physically. Lee and Kim (1976) have introduced such terms as a correction to the inviscid KdV equation occurring in free-surface hydrodynamics. In their theory the term accounts for the no-slip boundary condition of the viscous theory. However, it is not necessary to have a physical argument to justify the perturbation of the original problem introduced here. It suffices to say that the attached terms are mathematical in nature and produce a convergent algorithm for supercritical flows. Presumably, as the artificial viscosity parameters are reduced to zero, the correct approximate solution is retrieved.

Introducing a finite-difference model for the time variation in (4.6) in association with a time step Δt, we obtain the first iterative scheme to be studied here, which takes the following form:

$$\frac{\alpha}{\Delta t}(u^{n+1} - u^n) = \left[K_1 u^{n+\frac{1}{2}} - \frac{K_2}{2} u^n u^{n+\frac{1}{2}}\right]_{,x} + v_{,y}^{n+\frac{1}{2}} + \gamma u_{,xx}^{n+\frac{1}{2}} - \chi u^{n+\frac{1}{2}} \ ,$$

$$\frac{\beta}{\Delta t}(v^{n+1} - v^n) = u_{,y}^{n+1} - v_{,x}^{n+\frac{1}{2}} + \lambda v_{,yy}^{n+\frac{1}{2}} - Fv^{n+\frac{1}{2}} \ , \tag{4.7}$$

where, for example,

$$W^{n+\frac{1}{2}} = \frac{W^{n+1} + W^n}{2} \ .$$

Algorithm (4.7) has a linearization that is stable and second-order accurate. However, the nonlinear algorithm is not unconditionally stable. Certain minimum amounts of artificial viscosity as well as restrictions on the time step Δt are required to stabilize the algorithm. Note that the use of (4.7) requires the solution of an asymmetric linear system at each iteration.

We can obtain a second algorithm by treating the nonlinear term in (4.6) differently, as follows:

$$\frac{\alpha}{\Delta t}(u^{n+1} - u^n) = \left[K_1 u^{n+\frac{1}{2}} - \frac{K_2}{2}(u^{n+\frac{1}{2}})^2\right]_{,x} + v^{n+\frac{1}{2}}_{,y} + \gamma u^{n+\frac{1}{2}}_{,xx} - \chi u^{n+\frac{1}{2}} \quad , \tag{4.8}$$

$$\frac{\beta}{\Delta t}(v^{n+1} - v^n) = u^{n+\frac{1}{2}}_{,y} - v^{n+\frac{1}{2}}_{,y} + \lambda v^{n+\frac{1}{2}}_{,yy} - F v^{n+\frac{1}{2}} \quad .$$

Algorithm (4.8) is unconditionally stable; however, it requires the solution of a nonlinear system at each time step; thus, computationally is not as attractive as (4.7).

The third algorithm to be considered is obtained by constructing an explicit form of (4.6). It takes the following form:

$$\frac{\alpha}{\Delta t}(u^{n+1} - u^n) = \left[K_1 u^n - \frac{K_2}{2}(u^n)^2\right]_{,x} + v^n_{,y} + \gamma u^n_{,xx} - \chi u^n \quad . \tag{4.9}$$

$$\frac{\beta}{\Delta t}(v^{n+1} - v^n) = u^n_{,y} - v^n_{,x} + \lambda v^n_{,yy} - F v^n \quad .$$

This algorithm is only conditionally stable. In addition, certain minimum amounts of artificial viscosity are required to stabilize the nonlinear term. However, in some cases the computational simplicity of this algorithm may be advantageous.

The characteristic feature of these algorithms is the introduction of explicit artificial damping terms in both space and time for stability and convengence considerations. The accuracy of the solution depends, of course, on the size of these additional terms. For example, the inviscid solution can be retained only if the viscous term is of the same order as the truncation error. Similarly, the steady-state solution is accurate only if the terms proportional to u and v, which were introduced to dampen the iterative solution, are small. (These terms can be varied with iteration and gradually vanish when the solution reaches the steady state.) The explicit introduction of these terms facilitates the analysis and implementation of finite elements.* Moreover the coefficient of the damping terms may be chosen to optimize the rate of convergence.

---

*For example, instead of searching for a finite-element analog for the backward differencing of u_x, we explicitly add u_{xx} to it and use the usual Galerkin method (equivalent to centered differences for rectangular elements).

For unsteady problems, however, the transient solution is of primary concern. the same algorithm can be used with proper choice of different parameters. For example, if we wish to simulate the transonic low-frequency equation, β must vanish or at least be of the same order as the truncation error, namely $(\Delta t)^2$. The damping terms in time will harm the solution and therefore must be minimized. The main objective in the choice of these different parameters is, in this case, to minimize the phase error.

The explicit introduction of these "artificial" terms enables the algorithm to cope with completely different requirements. Obviously, this flexibility is advantageous in the study of unsteady transonic flows.

4.4 The Weak Formulation

Let $L_2(\Omega)$ be the space of square integrable functions on Ω . An inner product involving the functions of $L_2(\Omega)$ is defined as follows:

$$u,v = \int_\Omega uv \, dx \, dy \ .$$

The natural norm associated with $L_2(\Omega)$ is $||u||^2_{L_2(\Omega)} = u,u$. Let $L_\infty(\Omega)$ be the space of functions with the following norm:

$$||u||_{L_\infty(\Omega)} = \operatorname*{ess.\,sup.}_{\underset{\sim}{x} \in \Omega} |u(\underset{\sim}{x})| \ .$$

In addition, let $H^1(\Omega)$ be the Sobolev space with norm

$$||u||^2_{H^1(\Omega)} = ||u||^2_{L_2(\Omega)} + ||u_{,x}||^2_{L_2(\Omega)} + ||u_{,y}||^2_{L_2(\Omega)} \ .$$

A weak form of the system of partial differential equations (4.7) can be defined as follows: Find $u^{n+1}, v^{n+1} \in H^1(\Omega)$ such that

$$\begin{aligned} \frac{\alpha}{\Delta t}\, u^{n+1} - u^n, W &= K_1 u^{n+\frac{1}{2}} - \frac{K_2}{2} u^n u^{n+\frac{1}{2}}{}_{,x}, W \\ &\quad + v^{n+\frac{1}{2}}_{,y}, W + \gamma\, u^{n+\frac{1}{2}}_{,xx}, W - \chi\, u^{n+\frac{1}{2}}, W \ , \\ \frac{\beta}{\Delta t}\, v^{n+1} - v^n, S &= (u^{n+1}_{,y}, S) - (v^{n+\frac{1}{2}}_{,x}, S) \qquad (4.10) \\ &\quad + \lambda\, v^{n+\frac{1}{2}}_{,yy}, S - F\, v^{n+\frac{1}{2}}, S \ , \end{aligned}$$

for arbitrary $W,S \in H^1_o(\Omega)$, where $H^1_o(\Omega)$ is the space of functions in

$H^1(\Omega)$ that are zero on the boundary $\partial\Omega$. Integrating by parts in assorted terms on the right in (4.10) and using the fact that W and S are zero on the boundary, we obtain the following expression:

$$\frac{\alpha}{\Delta t}\left\langle u^{n+1} - u^n, W\right\rangle = -\left\langle\left[K_1 u^{n+\frac{1}{2}} - \frac{K_2}{2} u^n u^{n+\frac{1}{2}}\right], W_{,x}\right\rangle$$

$$+\left\langle v^{n+\frac{1}{2}}_{,y}, W\right\rangle - \gamma\left\langle u^{n+\frac{1}{2}}_{,x}, W_{,x}\right\rangle - \chi\left\langle u^{n+\frac{1}{2}}, W\right\rangle,$$

$$\frac{\beta}{\Delta t}\left\langle v^{n+\frac{1}{2}} - v^n, S\right\rangle = \left\langle u^{n+\frac{1}{2}}_{,y}, S\right\rangle - \left\langle v^{n+\frac{1}{2}}_{,x}, S\right\rangle \qquad (4.11)$$

$$- \lambda\left\langle v^{n+\frac{1}{2}}_{,y}, S_{,y}\right\rangle$$

$$- F\left\langle v^{n+\frac{1}{2}}, S\right\rangle$$

for all $W,S \in H^1_o(\Omega)$. Equation (4.11) represents the weak form of (4.7) in a conservative form, which is appropriate for the problem (4.1) and which naturally involves shocks.

A weak form of the system (4.8) can be developed using similar techniques. The following form is obtained:

$$\frac{\alpha}{\Delta t}\left\langle u^{n+1} - u^n, W\right\rangle = -\left\langle\left[K_1 u^{n+\frac{1}{2}} - \frac{K_2}{2}(u^{n+\frac{1}{2}})^2\right], W_{,x}\right\rangle$$

$$+\left\langle v^{n+\frac{1}{2}}_{,y}, W\right\rangle - \gamma\left\langle u^{n+\frac{1}{2}}_{,x}, W_{,x}\right\rangle - \chi\left\langle u^{n+\frac{1}{2}}, W\right\rangle,$$

$$\frac{\beta}{\Delta t}\left\langle v^{n+1} - v^n, S\right\rangle = \left\langle u^{n+\frac{1}{2}}_{,y}, S\right\rangle - \left\langle v^{n+\frac{1}{2}}_{,x}, S\right\rangle \qquad (4.12)$$

$$- \lambda\left\langle v^{n+\frac{1}{2}}_{,y}, S_{,y}\right\rangle - F\left\langle v^{n+\frac{1}{2}}, S\right\rangle,$$

for all $W,S \in H^1_o(\Omega)$. A weak expression of the same form can also be developed for (4.9).

A stability and convergence proof for the iterative techniques has been studied in detail by Wellford and Hafez (1977).

4.5 Finite-Element Models

In the numerical results to be presented here, we use algorithm (4.11). To implement this weak formulation, we subdivide the domain

Ω into finite elements Ω_e. Then Ω is $\bigcup_{e=1}^{E} \Omega_e$, where E is the total number of elements in the domain. On each domain Ω_e the velocity components U and V are approximated by a finite-element model of the following form:

$$U_e = \psi_i(x,y)U_i \ ,$$
$$V_e = \psi_i(x,y)V_i \ , \tag{4.13}$$

where $\psi_i(x,y)$ are finite-element interpolation (shape) functions, and U_i and V_i are the values of u and v at the nodes of the element. Of course, u and v could be interpolated with different shape functions; however, this procedure does not seem to present any advantage in this application. In the numerical results to be presented here, the eight-node serendipity element was used. In particular, the mesh used in this study is shown in figure 5. While, in this mesh each element has two sides parallel to the y coordinate axis, the method demonstrated here should also be valid for more general mesh configurations because the governing equations are hyperbolic at all points in the domain.

An approximate version of the weak formulation (4.11) is obtained by replacing u and v by U_e and V_e from (4.13) and setting $W = S = \psi_j$. This technique is simply the Galerkin method with the finite-element interpolation functions as trial functions. The following equations are obtained for a single element Ω_e:

$$(\alpha + \tfrac{\chi\Delta t}{2})K_{ij}U_i^{n+1} + \tfrac{\Delta t}{2} K_i B_{ji} U_i^{n+1} - \tfrac{\Delta t K_2}{4} C_{kij} U_k^n U_i^{n+1} - \tfrac{\Delta t}{2} D_{ij} V_i^{n+1} + \tfrac{\gamma\Delta t}{2} E_{ij} U_i^{n+1}$$
$$= (\alpha - \tfrac{\chi\Delta t}{2})K_{ij}U_i^n - \tfrac{\Delta t K_1}{2} B_{ji} U_i^n + \tfrac{\Delta t K_2}{4} C_{kij} U_k^n U_i^n + \tfrac{\Delta t}{2} D_{ij} V_i^n - \tfrac{\gamma\Delta t}{2} E_{ij} U_i^n$$

$$(B + \tfrac{\Delta t F}{2})K_{ij}V_i^{n+1} - \tfrac{\Delta t}{2} D_{ij} U_i^{n+1} + \tfrac{\Delta t}{2} B_{ij} V_i^{n+1} + \tfrac{\Delta t\epsilon}{2} E_{ij} V_i^{n+1} + \tfrac{\Delta t\lambda}{2} F_{ij} V_i^{n+1}$$
$$= (B - \tfrac{\Delta t F}{2})K_{ij}V_i^n + \tfrac{\Delta t}{2} D_{ij} U_i^n - \tfrac{\Delta t}{2} B_{ij} V_i^n - \tfrac{\Delta t}{2} \epsilon E_{ij} V_i^n - \tfrac{\Delta t}{2} \lambda F_{ij} V_i^n \ ,$$

where

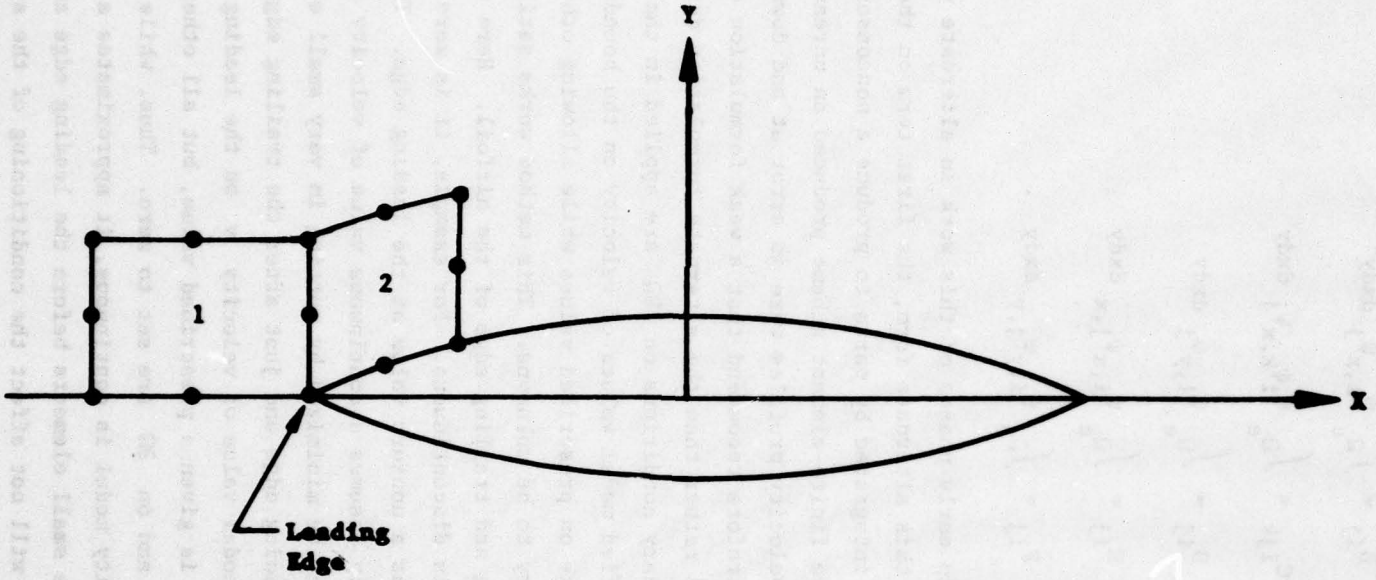

Figure 5. Mesh Spacing

$$K_{ij} = \int_{\Omega_e} \psi_i \psi_j \, dxdy$$

$$B_{ij} = \int_{\Omega_e} \psi_{i,x} \psi_j \, dxdy$$

$$C_{ijk} = \int_{\Omega_e} \psi_i \psi_{k,x} \psi_j \, dxdy$$

$$D_{ij} = \int_{\Omega_e} \psi_{i,y} \psi_j \, dxdy$$

$$E_{ij} = \int_{\Omega_e} \psi_{i,x} \psi_{j,x} \, dxdy$$

$$F_{ij} = \int_{\Omega_e} \psi_{i,y} \psi_{j,y} \, dxdy \quad .$$

We note that in early phases of this work an alternate version of (4.11) was used. In this alternate form, the first term on the right-hand side in (4.11) was integrated by parts to produce a nonconservative form. The nonconservative finite-element scheme produced an unreasonable answer. The computed velocity profiles were in error at and downstream of the shock. We therefore recommend that a weak formulation of the form of (4.11) be used rather than the alternate formulation described above.

The boundary conditions on $\partial\Omega$ are applied in the standard way by setting specified model values of velocity on the boundary either to be zero or to take on prescribed values while allowing other model velocities on the boundary to be unknowns. This method works satisfactorily except at the leading and trailing edge of the airfoil. Here the specified velocity v is discontinuous. For example, it is zero in front of the airfoil but has a nonzero value at the leading edge. The finite element model naturally assumes a continuous value of velocity everywhere. This discrepency can be minimized by putting in very small elements just before the leading edge and just after the trailing edge. Then, for example, the nodal value of velocity v on the leading edge in the small element is given a prescribed value, but all other nodes in the small element and on $\partial\Omega$ are set to zero. Thus, while the finite-element velocity model is continuous, it approximates a step function. Hopefully, the small elements before the leading edge and after the trailing edge will not affect the conditioning of the system.

We also tried an alternate procedure in this work. In assembly of the elements just upstream and downstream of the leading and trailing

edges, a special procedure was used. The compatibility of model velocities v at the leading edge and trailing edge was never enforced. Then, for example, in the element to the left of the leading edge, the nodal value of v at the leading edge was set to zero while, in the element to the right of the leading edge, the nodal value of v at the leading edge was given a prescribed value. This method did not produce satisfactory results. Apparently, the lack of compatibility in the four elements involved distorting the solution near the leading and trailing edges.

Test calculations were performed to determine the flow about a 6-percent parabolic arc airfoil. The mesh used is shown in figure 6. In the results to be presented here, $M_\infty = 0.875$ and $\gamma = 1.4$ while $\alpha = \beta = \gamma = \chi = \lambda = F$. The viscosity parameter α was given several values to demonstrate the convergence of the solution with decreasing viscosity. In figure 3 the approximate C_p distribution on the airfoil is pictured for $\alpha = 0.01$. The finite-element calculations are compared with the finite-difference results of Murman (1971, 1975) for $K = 1.8$. Table IV shows the convergence properties of the solution for $\alpha = 0.07$. The pointwise value of model velocity u at the point on the airfoil of maximum model velocity u of the converged solution is shown for the iterative steps. A variable time step was used, and this time step is indicated in the table. Convergence occurs after five iterative steps. After the fifth step, the algorithm seems to oscillate slightly about the solution. Depending on how strict the convergence criterion is, this oscillation may cause an increased number of iterations. Incorporation of a damping term involving a time derivative should eliminate this oscillation, although this method has not been used in this work.

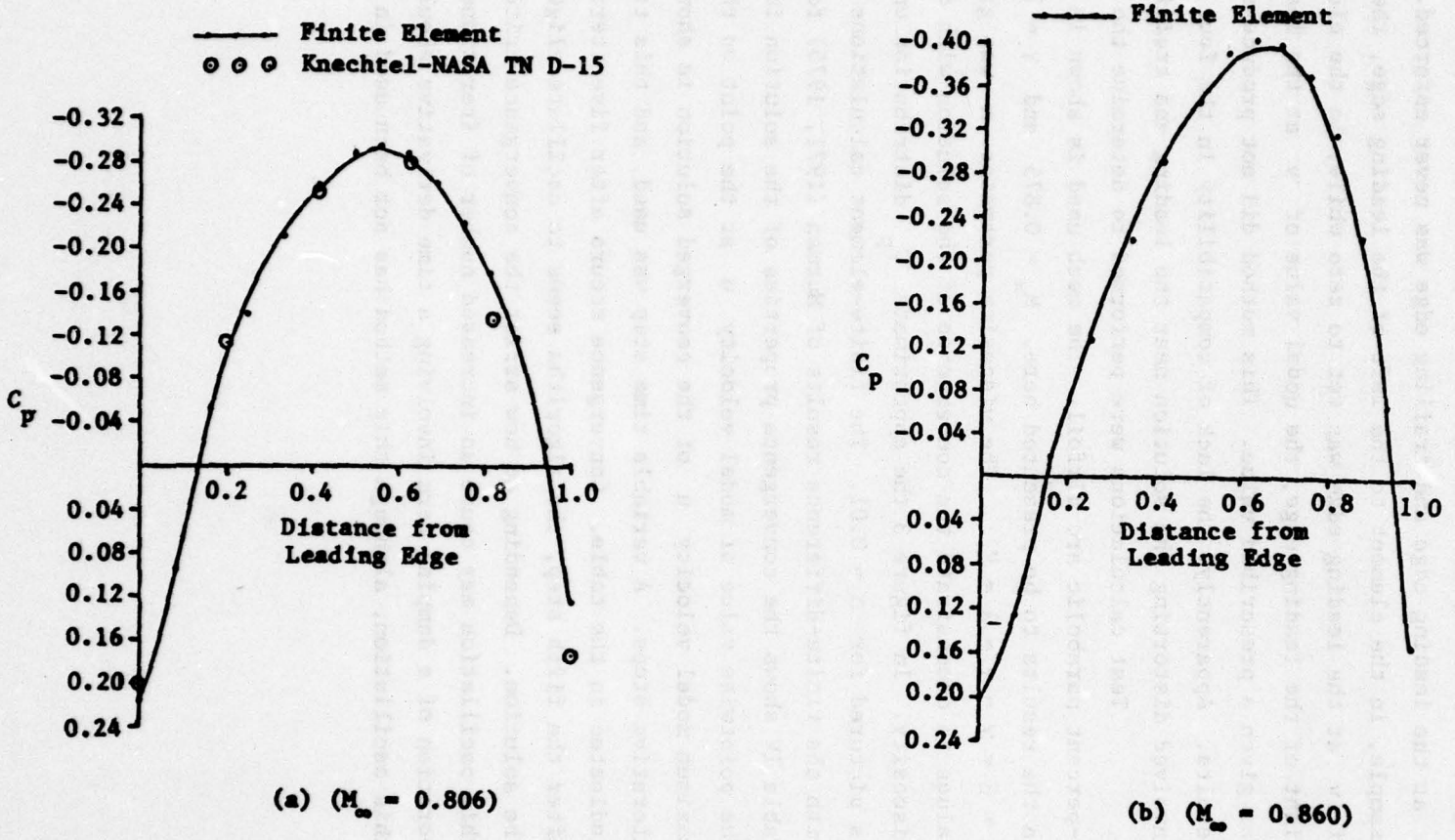

Figure 6. Six Percent Parabolic Arc Airfoil

TABLE IV: CONVERGENCE PROPERTIES OF THE APPROXIMATION FOR $\alpha = 0.07$.

Iteration Step	u Velocity Component	Time Step
1	0.07714	0.025
2	0.10730	0.025
3	0.11309	0.025
4	0.12995	0.1
5	0.13476	0.1
6	0.13409	0.1
7	0.13461	0.1
9	0.13481	0.1
11	0.13496	0.1

Note: u velocity components represent the velocity at the ninth node from the leading edge on the airfoil.

4.6 Conclusions

A hyperbolic system (in time) of first-order equations is used to calculate both steady and unsteady flows in a manner similar to Magnus and Yoshihara's time-dependent method. First, the time derivatives are discretized by using finite-differences of implicit Crank-Nicholson type. The resulting equations are linearized with Newton's method. Regularization techniques are needed for stability, as well as for the treatment of shock waves. Different artificial viscosity terms are added. Then, the space derivatives are discretized with a Galerkin finite-element procedure. Stability and convergence of the algorithm are analyzed, finite-element implementation of the transonic small-disturbance case is discussed, and a numerical example of flow around a parabolic arc airfoil is compared to Murman's finite-difference calculations. Preliminary results indicate that additional work is needed to assess the validity, applicability, and efficiency of the algorithm.

APPENDIX A: PARAMETRIC EXTRAPOLATION METHODS FOR THE SOLUTION OF THE HELMOHOLZ AND TRANSONIC HARMONIC PERTURBATION EQUATIONS

In this appendix we consider the frequency appearing in the perturbation equation as a parameter and approximate the behavior of the solution depending on this parameter.

Consider the one-dimensional exmaple:

$$\phi_{xx} + \omega^2\phi = 0$$

(with the exact solution $\phi = \sin \omega x$).

For small values of ω, the solution can be obtained by relaxation, say $\phi(\omega_1)$, $\phi(\omega_2)$, and $\phi(\omega_3)$. If we assume an expansion of ϕ in ω,

$$\phi(\omega) = \phi(\omega_o) + \frac{\partial\phi}{\partial\omega}(\omega_o)(\omega - \omega_o) + \frac{\partial^2\phi}{\partial\omega^2}(\omega_o)\frac{(\omega - \omega_o)^2}{2} + \cdots ,$$

where $$\frac{\partial\phi}{\partial\omega}(\omega_o) \simeq \frac{\phi(\omega_1) - \phi(\omega_3)}{\omega_1 - \omega_3} , \qquad \omega_o = \omega_2 = \frac{\omega_3 + \omega_1}{2}$$

$$\frac{\partial^2\phi}{\partial\omega^2}(\omega_o) \simeq [\phi(\omega_3) - 2\phi(\omega_2) + \phi(\omega_1)] / [(\omega_1 - \omega_3)/2]^2 .$$

Hence, an approximate solution $\bar{\phi}$ may be calculated at higher values of ω in terms of $\phi(\omega_1)$, $\phi(\omega_2)$, and $\phi(\omega_3)$.

A better approximation can then be calculated from (*)

$$\phi_{xx} = -\omega^2\bar{\phi} .$$

For this example, we have

---

*Note that the iterative procedure

$$\phi_{xx}^{n+1} = -\omega^2\phi^n$$

is divergent for $\omega > \omega_{cr}$ (since it can be described by the time-dependent equation $\phi_{xx} + \omega^2\phi = \omega^2\phi_t$).

$$\phi_{xx} = -\omega^2 \left| \sin \omega_o x - x \left[\cos(\omega_o x)\right](\omega - \omega_o) + x^2 \left[\sin(\omega_o x)\right](\omega - \omega_o)^2/2 \right| .$$

Obviously, the polynomial approximation (Taylor or Chebyshev) of the sinusoidal behavior is valid with some restrictions, which may not exclude using this method for the practical application of relaxation programs beyond the critical frequency.

An exponential approximation may be preferred; namely (Shanks Formula):

$$\phi(\omega) = \frac{\phi^o\phi^2 - (\phi^1)^2}{\phi^o + \phi^2 - 2\phi^1} \quad , \text{ where } \begin{cases} \phi^o = \phi(\omega_o) \\ \phi^1 = \phi(\omega_o) + \phi_\omega(\omega_o)(\omega - \omega_o) \\ \phi^2 = \phi(\omega_o) + \phi_\omega(\omega_o)(\omega - \omega_o) \\ \qquad + \phi_{\omega\omega}(\omega_o)\dfrac{(\omega - \omega_o)^2}{2} \end{cases}$$

The harmonic (Fourier) approximation gives the exact answer in this case if we use three sets of data to determine the amplitude, phase, and frequency; i.e., $\phi(\omega) = A \sin(\alpha\omega_i + \beta)$, $i = 1,2,3$.

For the two-dimensional, transonic harmonic perturbation, we can obtain the solution of the following equation for different (small values of ω by relaxation techniques:

$$(K - \phi^o_x)\phi^1_{xx} + \phi^1_{yy} - (\phi^o_{xx} + 2i\omega)\phi^1_x = 0 \quad .$$

Then, we obtain an estimate of the solution $\bar{\phi}$ for the required (high) value of ω by using a polynomial, exponential, or Fourier approximation. The final answer can then be obtained from the solution of

$$(K - \phi^o_x)\phi^1_{xx} + \phi^1_{yy} - \phi^o_{xx}\,\phi^1_x = 2i\omega\bar{\phi}_x \quad .$$

APPENDIX B: PROCEDURE FOR CALCULATING PRESSURES IN THE SHOCK REGION

Assume form of solution

$$\phi(x,y,t) = \phi^o(x,y) + \varepsilon e^{i\omega t}\phi^1(x,y) \tag{A2.1}$$

$$\phi_x(x,y,t) = \phi_x^o(x,y) + \varepsilon e^{i\omega t}\phi_x^1(x,y) \tag{A2.2}$$

$$X^D(y,t) = X^o(y) + \varepsilon e^{i\omega t}X^1(y) \tag{A2.3}$$

We assume that the solutions for the steady problem and perturbation problem are known. The pressure in the region of the shock must now be calculated.

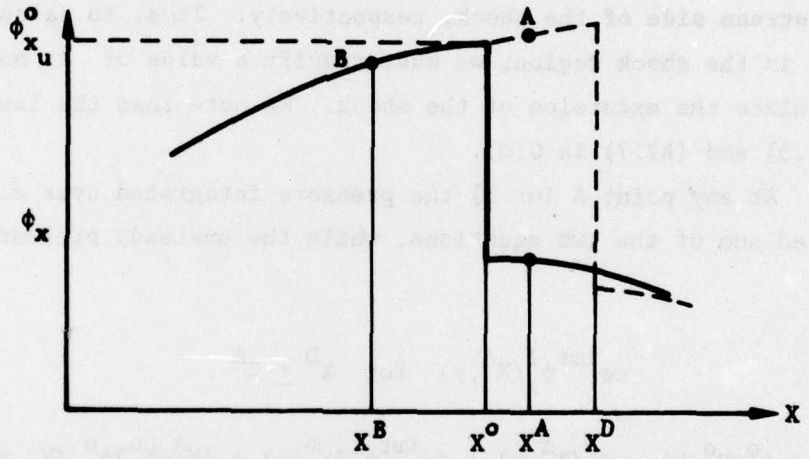

We consider a point A on the downstream side of the steady shock. If the perturbed shock at time t is upstream of X^A, the velocity is given as:

$$\phi_x(X^A,y,t) = \phi_x^o(X^A,y) + \varepsilon e^{i\omega t}\phi_x^1(X^A,y) \tag{A2.4}$$

$$\text{for } X^o \leq X^D \leq X^A \ .$$

If the perturbed shock at time t is downstream of X^A, the velocity is given as,

$$\phi_X(X^A,y,t) = \phi_x^o(X_u^o,y) + \varepsilon e^{i\omega t}\phi_x^1(X_u^o,y) + (X^A-X^o)\phi_{xx}^o(X_u,y) \tag{A2.5}$$

$$\text{for } X^o \leq X^A \leq X^D \quad .$$

Similarly, for a point B on the upstream side of the steady shock

$$\phi_x(X^B,y,t) = \phi_x^o(X^B,y) + \varepsilon e^{i\omega t}\phi_x^1(X^B,y) \tag{A2.6}$$

$$\text{for } X^B \leq X^D \leq X^o$$

and

$$\phi_x(X^B,y,t) = \phi_x^o(X_d^o,y) + \varepsilon e^{i\omega t}\phi_x^1(X_d^o,y) + (X^B-X^o)\phi_{xx}^o(X_d^o,y) \tag{A2.7}$$

$$\text{for } X^D \leq X^B \leq X^o \ ,$$

where X_u^o and X_d^o denote positions on the upstream side of the shock and the downstream side of the shock, respectively. Thus, to calculate the pressure in the shock region, we must specify a value of ε so that we can calculate the excursion of the shock. We note that the last term in eqs. (A2.5) and (A2.7) is $O(\varepsilon)$.

At any point A (or B) the pressure integrated over a cycle is a weighted sum of the two equations, while the unsteady pressure is given as:

$$\varepsilon e^{i\omega t}\phi_x^1(X^A,y) \quad \text{for} \quad X^D \leq X^A \tag{A2.8a}$$

$$\phi_x^o(X_u^o,y) - \phi_x^o(X^A,y) + \varepsilon e^{i\omega t}\phi_x^1(X_u^o,y) + (X^A-X^o)\phi_{xx}^o(X_u,y) \tag{A2.8b}$$

$$\text{for } X^D \geq X^A \quad .$$

Thus, when the shock passes over point A, there is a dramatic jump in the pressure, as would be expected.

Now, we compute the equivalent unsteady pressure at X^A by integrating over one cycle of oscillation of period $T = \frac{2\pi}{\omega}$.

$$\int_o^T \phi_x(X^A,y,t)dt = \int_o^T \phi_x^o(X^A,y)dt + \varepsilon \int_o^T e^{i\omega t}\phi_x^1(X^A,y)dt$$

$$= \int_{T_o}^{T_1} \left[\phi_x^o(X^A,y) + \varepsilon e^{i\omega t}\phi_x^1(X^A,y)\right] dt \qquad \text{(A2.9)}$$

$$+ \int_{T_1}^{T_2} \left[\phi_x^o(X_u^o,y) + \varepsilon e^{i\omega t}\phi_x^1(X_x^o,y)\right.$$

$$\left. + (X^A - X^o)\phi_{xx}^o(X_u^o,y)\right] dt$$

$$+ \int_{T_2}^{T} \left[\phi_x^o(X^A,y) + \varepsilon e^{i\omega t}\phi_x^1(X^A,y)\right] dt$$

where during the time T_1 to T_2 the shock is downstream of point A. Rewriting this equation, we get

$$\overline{\phi^o(X^A,y)T} + \varepsilon\overline{\phi^1(X^A,y)}\left(\frac{-iT}{2\pi}\right) = \phi_x^o(X^A,y)T$$

$$+ \left[\phi_x^o(X_u^o,y) - \phi_x^o(X_A,y) + (X^A - X^o)\phi_{xx}^o(X_u^o,y)\right](T_2 - T_1)$$

$$+ \varepsilon\left|\phi_x^1(X_A,y)\left(\frac{-i\pi}{2\pi}\right) + \left[\phi_x^1(X_o^u,y) - \phi_x^1(X^A,y)\right]\left(\frac{-i\pi}{2\pi}\right)e^{i\omega(T_2 - T_1)}\right| \qquad \text{(A2.10)}$$

Note that

$$\phi_x^o(X^A,y) = \phi_x^o(X_d^o,y) + (X^A - X^o)\phi_{xx}^o(X_d^o,y) \quad , \qquad \text{(A2.11)}$$

so the middle term becomes

$$\left|-\left[\!\left[\phi_x^o\right]\!\right]_{X^o} - (X^A - X^o)\left[\!\left[\phi_{xx}^o\right]\!\right]_{X^o}\right|(T_2 - T_1) \quad . \qquad \text{(A2.12)}$$

Thus, dividing through by T, we obtain

$$\overline{\phi_x^o}(X^A,y) - \varepsilon\frac{i}{2\pi}\overline{\phi_x^1(X^A,y)} = \phi_x^o(X_A,y) - \left[\!\left[\phi_x^o\right]\!\right]_{X_o}\left(\frac{T_2 - T_1}{T}\right)$$

$$- \varepsilon\frac{i}{2\pi}\left\{\phi_x^1(X^A,y) + \left[\phi_x^1(X_u^D,y) - \phi_x^1(X_D^A,y)\right] e^{i\omega(T_2-T_1)}\right.$$
$$\left. - i2\pi\left(\frac{X^A - X^o}{\varepsilon}\right)[\![\phi_{xx}^o]\!]_{X^o}\left(\frac{T_2 - T_1}{T}\right)\right\}, \qquad \text{(A2.13)}$$

and we see that,

$$\overline{\phi_x^o(X^A,y)} = \phi_x^o(X_A,y) - [\![\phi_x^o]\!]_{X_o}\left(\frac{T_2 - T_1}{T}\right) \qquad \text{(A2.14)}$$

$$\overline{\phi_x^1(X^A,y)} = \phi_x^1(X_A,y) + \left[\phi_x^1(X_u,y) - \phi_x^1(X_A,y)\right] e^{i\omega(T_2-T_1)}$$
$$- i2\pi\left(\frac{X^A - X^o}{\varepsilon}\right)[\![\phi_{xx}^o]\!]_{X^o}\left(\frac{T_2 - T_1}{T}\right). \qquad \text{(A2.15)}$$

The movement of the shock from the unsteady perturbation alters the mean or steady-state solution! It smooths out the discontinuity. A simple model of this was predicted by Tijdeman.

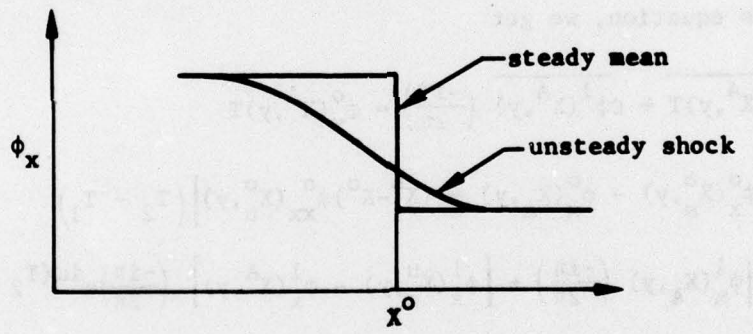

In addition, the unsteady pressure is altered by the shock motion.

The question is whether or not the second term belongs to the unsteady pressure contribution. It is formally of order (ε^o), but it arises out of the unsteady motion. We conclude that the lowest order unsteady solution is of order (ε^o) in a narrow region surrounding the steady-state shock position and of thickness $O(\varepsilon)$.

APPENDIX C: HARMONIC PERTURBATIONS OF UNSTEADY FULL POTENTIAL EQUATIONS

In this appendix, the problem of an oscillating airfoil is analyzed by using the full potential equation.

Governing Equations

A. Quasilinear Form:

$$(a^2 - u^2)\phi_{xx} - 2uv\phi_{xy} + (a^2 - v^2)\phi_{yy}$$

$$= 2u\phi_{xt} + 2v\phi_{yt} + \phi_{tt}$$

where $u = \cos\alpha + \phi_x$

$$v = \sin\alpha + \phi_y$$

$$a^2 = \frac{1}{M_\infty^2} - \frac{\gamma - 1}{2}\left[2\phi_t + u^2 + v^2 - 1\right]$$

and where u, v, and a have been normalized by the free-stream velocity U_∞.

B. Fully Conservative Form:

$$-\frac{\partial\rho}{\partial t} = \frac{\partial}{\partial x}(\rho u) + \frac{\partial}{\partial y}(\rho u)$$

where $\rho = \left[1 - \frac{(\gamma - 1)}{2} M_\infty^2 (2\phi_t + u^2 + v^2 - 1)\right]^{\frac{1}{\gamma - 1}}$

and where the density ρ has been normalized by the free-steam density ρ_∞.

Boundary Conditions

A. $F(x, y, t) = 0$ or $y - B(x, t) = 0$

$$\frac{DF}{Dt} = 0 \quad \text{or} \quad uF_x + vF_y = 0$$

$$(\phi_y)_B + \sin\alpha = \left[(\phi_x)_B + \cos\alpha\right] \cdot B_X + B_t$$

Let $B(x, t) = B^o(x) + B^1(x, t)$,

then $(\phi_y)_B + \sin\alpha = \left[(\phi_x)_B + \cos\alpha\right](B^o_x + B^1_x) + B^1_t$;

moreover, $(\phi_y)_B \simeq (\phi_y)_B{}^o$

$$(\phi_y)_B \simeq (\phi_x)_B{}^o \ .$$

B. In the far field, the mean steady-state value of ϕ is given in terms of the steady circulation Γ^o :

$$\phi = -\frac{\Gamma^o}{2\pi} \tan^{-1}\left[\sqrt{1 - M_\infty^2}\, \tan(\theta - \alpha)\right] \ .$$

The unsteady far-field formula may be obtained in terms of Kirchoff's formula. (Asymptotic expansion leads to a pulsating vortex for oscillation airfoils.)

Weak Solutions

The jump conditions admitted by the weak solutions are:

A. Shock Relations

B. Contact Surfaces (Wakes)

$$[\![\rho D_t + \rho u D_x + \rho v D_y]\!] = 0 \ ; \quad D(x, y, t) = 0$$

$$- D_t [\![\rho]\!] = D_x [\![\rho u]\!] + D_y [\![\rho v]\!] \qquad (43.1)$$

$$D(x, y; t) = x - x^s(y; t)$$

$$\frac{\partial x^s}{\partial t} [\![\rho]\!] = [\![\rho u]\!] - \frac{\partial x^s}{\partial y} [\![\rho v]\!]$$

(Conservation of mass across the shock)

From irrotationality conditions:

$$\phi_{tx} = \phi_{xt}$$

$$\phi_{ty} = \phi_{yt} \quad .$$

Hence $$D_t : D_x : D_y = [\![\phi_t]\!] : [\![\phi_x]\!] : [\![\phi_y]\!] \quad .$$

(A3.1) becomes

$$\frac{\partial x^s}{\partial t} [\![\rho]\!] = [\![\rho u]\!] + \frac{[\![\phi_y]\!]}{[\![\phi_x]\!]} [\![\rho u]\!] \quad ,$$

where $$\frac{\partial x^s}{\partial y} = - \frac{[\![\phi_y]\!]}{[\![\phi_x]\!]} \quad .$$

(Tangential velocity along the shock is preserved.)

(B) Across the wake, pressure is continous and so is ρ ; i.e.,

$$\rho \, [\![D_t + uD_x + vD_y]\!] = 0$$

(The relative velocity normal to the wake surface is zero.)

$$[\![p]\!] = 0.$$

In other words, $[\![\rho]\!] = 0$ or $[\![a^2]\!] = 0$

$$[\![2\phi_t + (\phi_x - \cos \alpha)^2 + (\phi_y - \sin \alpha)^2]\!] = 0$$

$$2[\![\phi_t]\!] + [\![\phi_x^2]\!] + 2 \cos \alpha \, [\![\phi_x]\!] + [\![\phi_y^2]\!]$$

$$+ 2 \sin \alpha \, [\![\phi_y]\!] = 0$$

<u>Simplifications</u>:

1. Assume the wake vorticles are located on the x axis.
2. Asssume ϕ_y is continous across the wake.

The Kutta and wake boundary conditions then become

$$[\![\phi_t]\!] + [\![\phi_x]\!](1 + \langle \phi_x \rangle) = 0 \; ; \; x \geq 1 \quad (y = 0)$$

$$(\alpha << 1) \quad .$$

An interesting problem would be to trace the wake and to use both relationships derived before.

Harmonic Perturbations

Let $$\phi = \phi^o(x, y) + \varepsilon \, \mathrm{Re}\left[e^{i\omega t} \, \phi^1(x, y)\right] + \cdots$$

$$X = X^o(x, y) + \varepsilon \, \mathrm{Re}\left[e^{i\omega t} \, X'(y)\right] + \cdots$$

where the boundary condition is

$$B(x, t) = B^o(x) + \varepsilon \, \mathrm{Re}\left[e^{i\omega t} \, B^1(x)\right] .$$

If we subsitute the expansion for ϕ into the differential equation and the jump conditions the zero-order problem is exactly the steady problem. The first-order problem ϕ^1 is the perturbation, where X^1 is the shock movement.

A shock fitting method for ϕ^1 is needed; otherwise we may use a fully conservative scheme in strained coordiantes as in the small-disturbance case.

Zeroth-Order Problem

Differential Equation: $$(a^{o^2} - u^{o^2})\phi^o_{xx} + 2u^o v^o \phi^o_{xy} + (a^{o^2} - v^{o^2})\phi^o_{yy} = 0$$

where $$u^o = \cos\alpha + \phi^o_x$$

$$u^o = \sin\alpha + \phi^o_y$$

$$a^{o^2} = \frac{1}{M_\infty^2} - \frac{\gamma - 1}{2}\left[u^{o^2} - v^{o^2} - 1\right]$$

Boundary Conditions: $$(\phi^o_y)_{B^o} + \sin\alpha = \left[(\phi^o_x)_{B^o} + \cos\alpha\right] B^o_x$$

Wake: $$[\![\phi^o_y]\!]_{y=0} = 0 \quad , \quad [\![\phi^o]\!] = \Gamma^o \quad ; \; x \geq 1$$

Far Field: $$\phi = -\frac{\Gamma^o}{2\pi}\tan^{-1}\left[\sqrt{1-M_\infty^2}\tan(\theta-\alpha)\right].$$

Jump Conditions: $$[\![\rho^o u^o]\!]_s - \left(\frac{\partial x^o}{\partial y}\right)_s [\![\rho^o u^o]\!]_s = 0$$

$$[\![\phi^o]\!]_s = 0$$

Jameson's Fully Conservative Schemes* or rotated schemes with shock fitting may be used to solve this problem.

First-Order Problem

Differential Equation: $$(a^{o2} - u^{o2})\phi^1_{xx} + 2u^o v^o \phi^1_{xy} + (a^{o2} - v^{o2})\phi^1_{yy} = \text{N.H.},$$

where N.H. stands for nonhomegeneous terms, which will not change the type of the equation.

Boundary Conditions: $$(\phi^1_y)_{B^o} = \left[\left(\phi^o_x\right)_{B^o} + \cos\alpha\right] B^1_x(x) + \left[\left(\phi^1_x\right)_{B^o}\right] B^o_x + i\omega B^1(x)$$

Wake: $$[\![i\omega\phi^1]\!]_{y=o} + [\![\phi^1_x]\!]_{y=0} + \left[\phi^o_x\right]_{y=0}\langle\phi^1_x\rangle_{y=0} + [\![\phi^1_x]\!]_{y=0}\langle\phi^o_x\rangle_{y=0} = 0$$

Far Field: $\phi^1 = 0$ (for the present time)

Jump Conditions:

1) $$[\![\phi^1]\!]_{x^o} = -X^1 [\![\phi^o_x]\!]_{x^o}$$

2) $$i\omega [\![\rho^o]\!]_{x^o} X^1 = [\![\rho^o u^1]\!]_{x^o} - \frac{\partial x^o}{\partial y}\left\{[\![\rho^o v^o]\!]_{x^o} + [\![\rho^1 v^o]\!]_{x^o}\right\} + [\![\rho^1 u^o]\!]_{x^o} - \frac{\partial x^1}{\partial y}[\![\rho^o y^o]\!]_{x^o}.$$

These jump conditions must be imposed on the ϕ^1 problem. A shock fitting procedure is necessary, where an ordinary differential equation in X^1 is

*In this case multiply the equation by $\rho^o/(a^o)^2$.

solved simultaneously with the partial differential equation of ϕ^1, given ϕ^o and X^o .

An alternative to the approach based on the method of strained coordinates may be used here, as in the small-disturbance case.

REFERENCES

Ballhaus, W. private communication.

Chan, S. T. K., Brashears, M. R., and Young, V. Y. C., (1975) "Finite Element Analysis of Transonic Flow by the Method of Weighted Residuals," AIAA Paper No. 75-79.

Cheng, H. K. and Hafez, M. M. (1973) "Equivalence Rule and Transonic Flows Involving Lift," AIAA Paper No. 73-88.

Dietrick, D., McDonald, B. E., and Warm-Varnas, A. (1975) "Optimized Block - Implicit Relaxation," Journal of Computational Physics 18, 421-439.

Glowinski, R., Periaux, J. and Pironneau, O. (1976) "Transonic Flow Simulation by the Finite Element Method Via Optimal Control," 2nd Intl. Symp. Finite Element Methods in Flow Problems, Rapallo, Italy, June.

Hafez, M. M., Murman, E. M., and Wellford, L. C. (1976) "Application of Finite Element Approach to Transonic Flow Problems," 2nd Intl. Symp. Finite Element Method in Flow Problems, Rapallo, Italy, June.

Isaacson, E., and Keller, H. B. (1966) Analysis of Numerical Methods, John Wiley & Sons.

Landahl, M. T. (1961) Unsteady Transonic Flow, Pergamon Press, Long Island City, N.Y.

Lee, J. J. and Kim, S. T. (1976) "A Viscous Model for Dispersive Long Waves," Abstracts of Papers at Fifteenth Conference on Coastal Engineering, July 11-17, 1976, Honolulu, Hawaii, pp. 692-694.

Lees, M. (1960) "A Priori Estimates for the Solution of Difference Approximations to Parabolic Partial Differential Equations," Duke Mathematical Journal 26, pp. 297-311.

Lions, J. L., and Mageres, E. (1972) Non-Homegeneous Boundary Value Problems and Applications, Springer-Verlag, New York.

Magnus, R. and Yoshihara, H. (1970) "Inviscid Transonic Flow Over Airfoils," AIAA Paper No. 70-47.

McAvaney, B. J. and Leslie, L. M. (1971) "Comments on a Direct Solution of Poisson's Equation by Generalized Sweep-Out Method," Journal of the Meteorological Society of Japan, vol. 50, no. 2.

Molberg, J. R. (1968) "Numerical Solutions to Maxwell's Equations" Ph.D. Thesis, University of Washington.

Murman, E. M., and Cole, J. D. (1971) "Calculations of Plane Steady Transonic Flows," AIAA J. 9, pp. 114-121.

Murman, E. M. (1975) "Analysis of Embedded Shock Calculated by Relaxation Methods," AIAA J. 12, pp. 626-633.

Nixon, D. (1977) "Perturbation of a Discontinuous Transonic Flow," AIAA Paper No. 77-206.

Oden, J. T. and Reddy, J. N. (1976) Mathematical Theory of Finite Elements, Wiley-Interscience, New York.

Traci, R. M., Abano, E. D., and Farr, J. L., Jr. (1975) "Perturbation Method for Transonic Flows About Oscillating Airfoils," AIAA Paper No. 75-877.

Weatherill, W. H., Ehlers, F. E., and Sebastian, J. H. (1975) "Computation of the Transonic Perturbation Flow Fields Around Two- and Three-Dimensional Oscillating Wings," NASA CR-2599.

Wellford, L. C. and Hafez, M. M. (1976) "Application of Finite Elements to Transonic Flow Problems," 2nd Intl. Symp. Finite Element Methods in Flow Problems, Rapallo, Italy, June.

Wellford, L. C. and Hafez, M. M. (1977) "An Implicit Velocity Formulation for the Small-Disturbance Transonic Flow Problem Using Finite Elements," Flow Research Report No. 81.

*U.S.Government Printing Office: 1978 — 757-080/339